RSC Advances

REVIEW

View Article Online
View Journal | View Issue

Cite this: *RSC Adv.*, 2022, **12**, 20264

Target-specific mononuclear and binuclear rhenium(I) tricarbonyl complexes as upcoming anticancer drugs

Ajay Sharma S., † Vaibhavi N., † Binoy Kar, Utpal Das and Priyankar Paira *

Metal complexes have gradually been attracting interest from researchers worldwide as potential cancer therapeutics. Driven by the many side effects of the popular platinum-based anticancer drug cisplatin, the tireless endeavours of researchers have afforded strategies for the design of appropriate metal complexes with minimal side effects compared to cisplatin and its congeners to limit the unrestricted propagation of cancer. In this regard, transition metal complexes, especially rhenium-based complexes are being identified and highlighted as promising cancer theranostics, which are endowed with the ability to detect and annihilate cancer cells in the body. This is attributed the amazing photophysical properties of rhenium complexes together with their ability to selectively attack different organelles in cancer cells. Therefore, this review presents the properties of different rhenium-based complexes to highlight their recent advances as anticancer agents based on their cytotoxicity results.

Received 2nd June 2022
Accepted 24th June 2022

DOI: 10.1039/d2ra03434d

rsc.li/rsc-advances

1. Introduction

The design of anticancer drugs with minimum or negligible side effects has been the focus of scientists to bring about a revolution in the field of anticancer research. Therefore, various ideas and attempts have been reported to design anticancer drugs, where transition metal-based complexes are emerging as highly effective anticancer agents in comparison to so-called anticancer organic drugs. It has been observed that cancer cells can readily adapt to micro changes in the environment, and also evade the role of growth suppressors in the body. Consequently, their replication rate is uncontrollably higher than the growth of normal non-cancerous cells in the body.[1] According to the report of the World Health Organization (WHO), 4.7 million women and 5.3 million men develop malignant tumours annually, resulting in the death of nearly 6.2 million people.[2] The treatment of cancer involves either the surgery of malignant cells or the application of well-known chemotherapy followed by radiation therapy. The

Department of Chemistry, School of Advanced Sciences, Vellore Institute of Technology, Vellore-632014, Tamil Nadu, India. E-mail: priyankar.paira@vit.ac.in; Fax: +91-416-2243092; Tel: +91-416-2243091

† Equal contribution.

Ajay Sharma S. graduated from the Vellore Institute of Technology, Vellore with a master's degree in organic chemistry. His previous research was based on ruthenium and iridium based anticancer scaffolds under the guidance of Dr Priyankar Paira and has also published articles in the same field. His research interest includes organometallic and medicinal chemistry.

Vaibhavi N. graduated from Christ University, Bangalore with a Bachelor's degree in Physics, Chemistry and Mathematics. She later completed her master's from Vellore Institute of Technology, Vellore with specialization in organic chemistry and is currently working as a project assistant at IIT Mandi. She has previously conducted research in the fields of materials chemistry, supramolecular chemistry and organic synthesis in various labs. She has worked under the guidance of Dr Priyankar Paira in the field of anticancer scaffolds and has published a review article in the same field.

chemotherapeutic treatment strategy is a salient approach for healing almost all types of cancer. However, a major disadvantage of chemotherapy is that it damages normal cells together with cancer cells, which results in many side effects such as ototoxicity (damage of inner ear), peripheral neuropathy, nephrotoxicity (toxicity in the kidney), hepatotoxicity (liver damage), cardiotoxicity (weakening of the heart), gastrointestinal toxicity, haematological toxicity, and hypersensitivity reactions (HSRs), which pose very serious health concerns.[3] Accordingly, a good anticancer drug should not impair normal cells and selectively attack cancer cells. In most cases, it has been observed that cancer cells acquire resistance towards anticancer drugs, which renders the drug inactive or incapable of reducing the tumour mass over time.[4] This fundamental drawback has now been addressed by researchers, leading to the development of transition metal complexes as anticancer agents. This is because transition metal complexes exhibit unique properties, which boost their anticancer activities in the cancerous environment. These metal complexes exhibit desirable photophysical properties, inertness, radioactivity, and preferential binding to cell organelles, which make them appropriate for diagnostic and therapeutic applications.[5] Metal complexes have a wide structural diversity due to their flexibility in adopting various types of shapes such as trigonal bipyramidal, square planar, square pyramidal, and octahedral. This allows them to be useful in effective binding interactions with target biomolecules. Additionally, it has been observed that transition metal complexes can interact with DNA reversibly,[6] which is significant in molecular biology and cancer research. Alternatively, the possibility of redox processes and ligand exchange occurring offers metal complexes unique reactivity, which is rare with the use of organic drug molecules.[7] One of the earliest clinically approved metal-based anticancer drug is cisplatin [*cis*-diamminedichloridoplatinum(II)]; however, it causes numerous side effects such as allergic reactions, kidney problems, haemorrhage and reduced immunity to infections[8] including the relapse of the disease.[9] Although the mechanism of action of cisplatin and its congeners has been observed to be damaging DNA and inducing apoptosis in cancer cells,[10] and they have also been clinically successful in the treatment of

Binoy Kar obtained his Bachelor of Science degree from Dinabandhu Andrews College, University of Calcutta, in 2017 and received his Master of Science degree from West Bengal State University (2019), with specialization in Organic Chemistry. He joined VIT Vellore, India, in December 2019 under the supervision of Dr Priyankar Paira and is pursuing his PhD, focusing on "Design, synthesis and characterization of novel organometallic anticancer drugs and study on their biological applications".

Utpal Das received a Bachelor of Science degree from West Bengal State University, India, in 2017 and Master of Science degree from West Bengal State University, India, in 2019 with specialization in Organic Chemistry. He is currently pursuing his PhD degree from Vellore Institute of Technology, Vellore, under the supervision of Dr Priyankar Paira. His research interest includes Organometallic and Bioinorganic Chemistry.

Dr Priyankar Paira completed his PhD from Indian Institute of Chemical Biology in the year 2010 and Post doc from National University of Singapore (2010–2013). He was appointed as Assistant Professor in Vellore Institute of Technology in 2013 and promoted to Sr. Assistant Professor in 2018. He has 12 years research experience after PhD in the field of bioinorganic and medicinal chemistry in VIT as well as in National University of Singapore. He has worked on A_3 adenosine receptor targeting novel phototoxic cancer cell markers. He has an established chemistry and biology lab in VIT to do the interdisciplinary work. He has 95 publications in reputed international journals in the field of bioinorganic and medicinal chemistry. He also has 3 patents in medicinal chemistry. He has a high citation (1443) and H. Index (20) because of his significant contribution in research. He successfully completed a DST-SERB-YS (YSS/2014/000842) project on A_3 receptor targeting novel organoruthenium scaffolds as cancer cell markers and its application in photodynamic therapy. He also has another DST-SERB project entitled, "Ru(II)-arene-2-aryl benzothiazole/benzoxazole, quinoxaline and phenanthroline analogues as fluorescent probes and cancer theranostics applications" (EMR/2017/000816) as Co-PI. Currently, he has one ongoing project from DST-SERB entitled "Emergence of mitochondria targeting Ir(III)/Re(I)based multinuclear complexes as cancer photo-theranostic agent" (CRG/2021/002267) as PI. Recently he was recognised as a MRSC and is also working as an active member of SBIC, ISC and ACS. In particular, he has always been fascinated by the research involving combination of engineering, medicine and science as demonstrated by his publications and collaboration with a number of people from different institutes having diverse research expertise. He is a reviewer for several RSC, ACS, Wiley and Elsevier journals. Currently he is appointed as editorial board member in Current Electrocatalysis, Bentham Science and Frontier in Chemistry.

lung, neck, head and genitourinary tract cancer,[11] their significant discrepancies have triggered further studies and the creation of metal-based anticancer scaffolds. However, the effort to replace cisplatin with more selective anticancer drugs is a significant challenge to researchers. In this case, metal complexes are emerging with significant selectivity, exhibiting surprising anticancer activities towards various types of cancers. The excellent selectivity of these metal complexes has become the focus of researchers in terms of simplifying targeted cancer therapy by avoiding the side effects and risks associated with post-chemotherapeutic treatment.[12–25] Among the transition metal complexes, rhenium (Re) organometallic complexes

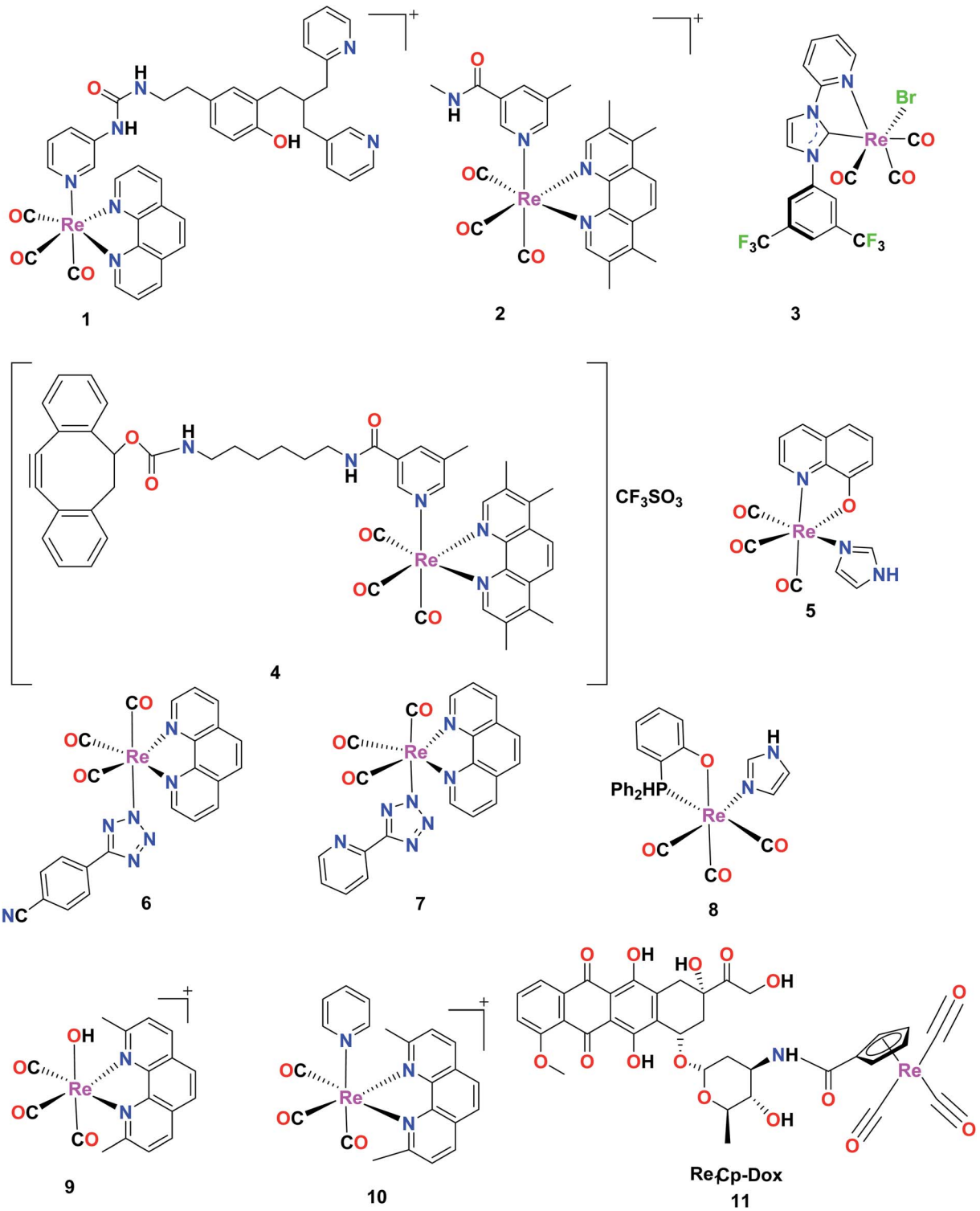

Fig. 1 Some reported rhenium complexes for anticancer applications.[29,42,47,49–53]

with the general formula fac-$Re(CO)_3$ exhibit remarkable properties including photo-redox stability, easy synthesis *via* one-step strategy, thermal and kinetic stability, and ionic or neutral complexes with remarkable CO stretching frequency.[24] The apparent C–O stretching frequency enables the use of these complexes for imaging studies[26] through IR and Raman spectroscopy.[27] Commonly, Re(I) tricarbonyl complexes are seen to exhibit sharp peaks at 1800–2200 cm^{-1} in their infrared spectrum. These complexes exhibit excellent photochemical, photophysical, luminescent properties,[28] and also offer different mechanisms of action such as photoactivity, redox activity, ligand exchange and catalytic activity.[29,30] Furthermore, their advantages of large Stokes shift, long-lived excited states, resistance to photo-bleaching, and also high quantum yield amplify the range of applications of these complexes in this field.[31] They are biologically active and have the potential to be utilized as targeted drugs in cancer therapy.[32] Consequently, these complexes are emerging as promising anticancer agents, which can be a viable alternative to platinum-based anticancer drugs[33] for application in medicinal chemistry.[34] Re exhibits variable oxidation states (−3, −1, +1, +2, +3, +4, +5, +6, and +7), and thereby delivers noteworthy and unique properties[35] in the realm of transition metals. It is very interesting to mention that in its lower oxidation states, rhenium is hardly affected by the reactive species present in its chemical environment.[36] Rhenium has 2 radioisotopes (^{186}Re and ^{188}Re, which emit beta radiation), which are used in radionuclide therapy.[37] Specifically, antibody fragments, peptides, intact antibodies, DNA and oligomers have been labelled with the ^{188}Re isotope.[38] Isotopic oxo Re(V) complexes are important in radio-pharmaceutical medicine.[39] The ^{188}Re isotope is utilized in radio immunotherapy (RIT) due to the curtailed exposure to radiation because it emits beta and gamma rays with a short half-life (16.9 h).[40] Complexes containing chromophoric ligands are adroitly used in biological imaging,[41] as anionic sensors and also as light-induced anticancer agents.[42] In this case, the synthesis of these metal complexes is carried out stepwise, where the ligands are synthesised first, and subsequently coordinated to the metal.[43] Because rhenium(I) is a soft metal, it favours soft donors such as nitrogen, and hence tridentate metal complexes with nitrogen donors are common.[36] Diverse rhenium complexes can be synthesised *via* a wide range of ligand substitutions with ease.[44] They are also efficient as luminescent cell markers.[45] Re(I) tetrazolato complexes are used as luminescent staining agents for proteins.[46] The luminescent polypyridine rhenium complexes have long-lasting excited states and ^{3}MLCT (metal to ligand charge transfer) transitions, which are helpful in designing multicoloured probes (Fig. 1).[47] These complexes also have applications in nuclear imaging.[48] Rhenium complexes induce cell death by various methods such as necroptosis, apoptosis and paraptosis.[12] Their desirable properties make them suitable for use in photoactivated chemotherapy and/or photodynamic therapy.[48] After discussing the importance of rhenium complexes in cancer therapy, our review will focus on the significant rhenium organometallic and tricarbonyl complexes, highlighting their excellent cytotoxicity.

2. Rhenium(I) complexes

Rhenium complexes have shown promising results in the quest for potential anticancer drugs. The presence of a fluorescent ligand and metal ion of bioimaging relevance in rhenium organometallic complexes can be investigated for their biological activity. The ligand (L) has been varied and investigated by substituting different η^5 chelators, tridentate and bidentate ligands to explore and enhance its fluorescent and optical imaging properties.[54] It has been observed that complexes with tridentate ligands having a symmetrical nature possess lower bioaccumulation compared to complexes with monodentate or bidentate ligands.[36] They induce anticancer activity through various mechanisms, which are focused mainly on targeting cancer cell organelles, interaction with DNA, inhibition of enzymes and protein kinases, disruption of the activity of mitochondria, inducing cytoplasmic vacuolization and apoptosis.[55,56] In the subsequent sections of this study, we discuss the cytotoxicity of rhenium organometallic complexes, focusing mainly on rhenium tricarbonyl complexes and highlighting their potential as cancer theranostics.

Rhenium tricarbonyl monometallic complexes

Bipyridine and phenanthroline-based $Re^{(I)}(CO)_3$ complexes. Knopf *et al.* synthesized (Fig. 2a) a set of Re complexes, fac-$[Re(CO)_3(NN)(Cl)]$ **Re12(a–g)**, where NN represents diimine ligands, which exhibited poor solubility. Thus, aqua complexes of rhenium, fac-$[Re(CO)_3(NN)(OH_2)]^+$ **Re12(h–n)**, where NN = 2,2′-bipyridine (**Re12h**), 4,4′-dimethyl-2,2′-bipyridine (**Re12i**), 4,4′-dimethoxy-2,2′-bipyridine (**Re12j**), dimethyl 2,2′-bipyridine-4,4′-dicarboxylate (**Re12k**), 1,10-phenanthroline (**Re12l**), 2,9-dimethyl-1,10-phenanthroline (**Re12m**) and 4,7-diphenyl-1,10-phenanthroline (**Re12n**), were considered for further studies. The cytotoxicity results showed that **Re12c** was the most potent (IC_{50} = 3.0 μM), while the IC_{50} values of **Re12i** and **Re12j** were found to be less than 10 μM against HeLa cells by the MTT assay. Alternatively, the **Re12i**, **Re12j** and **Re12m** complexes showed promising results, and hence they were further tested against different cancer cell lines including KB-3-1, KBCP20, the ovarian cancer cell lines A2780 and A2780CP70, and the lung cancer cell lines A549, A549 CisR H460 and MRC5, where they revealed their good cytotoxicity profiles with IC_{50} values of less than 20 μM. Also, they exhibited lower resistance factors in comparison to cisplatin, indicating their ability to overcome the mechanisms that cause resistance to cisplatin. It was seen that **Re12m** was highly effective in all leukaemia cell lines tested, bringing out its intrinsic luminescence properties. The authors investigated the intracellular localization of the **Re12m** complex with the assistance of confocal fluorescence microscopy. The emission of **Re12m** was noticeable in the cells considerably above the background autofluorescence (Fig. 2b). The presence of cytoplasmic vacuoles was discovered, which appeared to be a rhenium complex effect. The vivid luminous exterior membranes of the vacuoles suggested the significant accumulation of the complex. This complex showed considerable metabolic stability, and also could induce caspase-independent

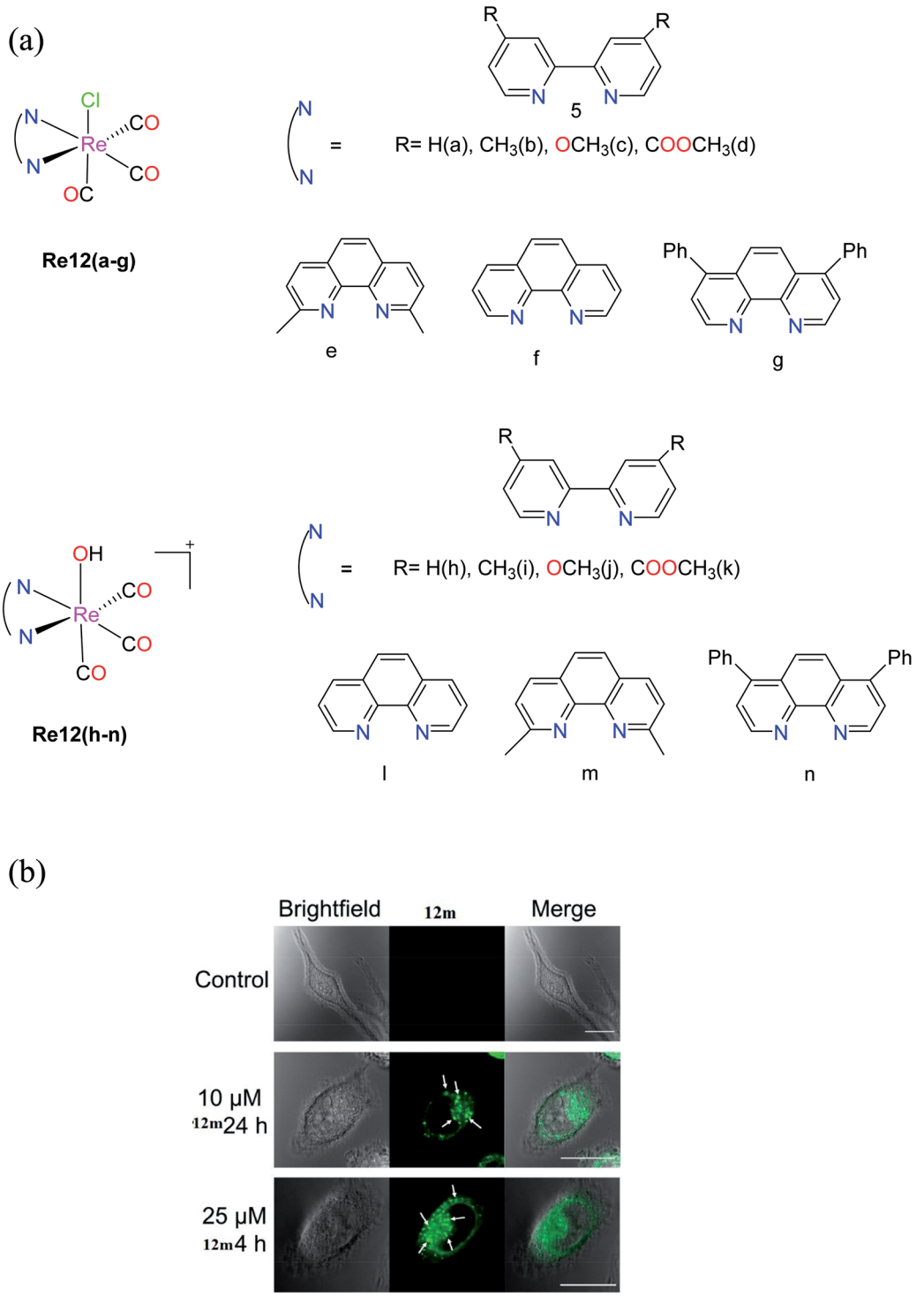

Fig. 2 (a) Structures of fac-$[Re(CO)_3(N{-}N)(OH_2)]^+$ complexes. (b) Brightfield and confocal fluorescent microscope images of control HeLa cells and HeLa cells treated with **12m**. Arrows point to vacuoles induced by **12m** treatment. Scale bars = 20 μm. [Adapted from ref. 26 with permission from the American Chemical Society.].

cell death accompanied by lysosome-dependent cytoplasmic vacuolization without increasing the generation of ROS.[26]

Organometallic rhenium(I) imine complexes

Osses *et al.* synthesized novel organometallic rhenium(I) imine complexes of the general formula $[(\eta^5\text{-}C_5H_4CH{=}N{-}(CH_2)_5{-}Pz{-}R)Re(CO)_3)]$, where Pz–R represents alkyl or aryl piperazine groups. These piperazine-based ligands are well-known to inhibit the GSK-3β kinase (glycogen synthase kinase 3). Therefore, biological toxicity studies were performed on the HT-29 and PT-45 cancer cell lines using these Re(I) imine complexes given that the GSK-3β kinase plays an important role in these

cancer cell lines. The **L4** ligand (NH_2–$(CH_2)_5$–Pz-1–CH–$(C_6H_5)_2$) and the Re(I) complex **Re13(a–b)**, where **Re1** = ([[(η^5-C_5H_4CH=N–$(CH_2)_5$–Pz–C_6H_{11})]]) and **Re2** = ([[(η^5-C_5H_4CH=N–$(CH_2)_5$–Pz–C_6H_5)]]), exhibited higher selectivity and activity against colon cancer cells compared to the standard drug cisplatin. The IC_{50} value of ligand **L4** was found to be 18.11 μM and 22.23 μM in the HT-29 and PT-45 cell lines, respectively. The **Re13d** ([(η^5-C_5H_4CH=N–$(CH_2)_5$–Pz-1–CH–$(C_6H_5)_2$]) complex showed a remarkable IC_{50} in the range of 30 μM against both the cell lines. It was concluded that an increase in the aromaticity of the organic ligands and the presence of an electron-donating substituent on the nitrogen atom of piperazine contributed to the effective cytotoxicity of the complexes on both the cell lines (Fig. 3).[32]

Konkankit *et al.* synthesized Re complexes bearing a pyridyl imine Schiff base ligand with different alkyl chains (Fig. 4a), and then their cytotoxicity was measured in HeLa cells. The IC_{50} values of these complexes were nearly 15 μM. The cytotoxicity of these complexes depends on the length of the alkyl chain, and hence **Re14f** having more alkyl chains induced an appreciable cytotoxic effect on a larger and faster scale compared to the other complexes. All the complexes were reported to be lipophilic in nature and the studies showed that more lipophilic compounds were competent to trigger cell death more rapidly than other hydrophobic analogues. Lipophilicity plays a mutually important role in the uptake and cytotoxicity of drug molecules. The log(P_a) values of the complex were observed to be **Re14a** (1.59), **Re14b** (2.16), **Re14c** (2.44), **Re14d** (2.80), **Re14e** (2.95), **Re14f** (2.95). Compounds having more lipophilicity can produce *in vitro* anticancer activities within a much shorter time.[33]

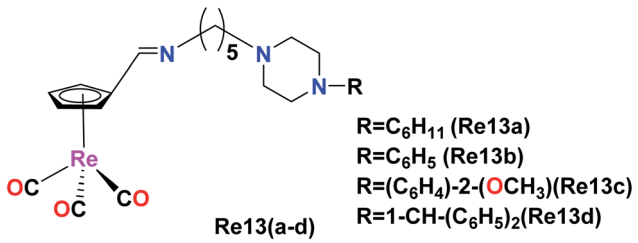

Fig. 3 Structure of Re complex with the formula [(η^5-C_5H_4CH=N–$(CH_2)_5$–Pz–R)Re$(CO)_3$].

Re(I) tricarbonyl NNN and NSO complexes

A tricarbonyl complex bearing a piperidinyl sulphonamide group (**Re15**) with the formula $[Re(CO)_3(N(SO_2pip)dpa)]^+$ and ligand ($N(SO_2pip)dpa$) was synthesized and reported by Subasinghe *et al.* These compounds were tested against a human breast cancer cell line (MCF-7). The IC_{50} of the ligand was 139 μM and the IC_{50} of complex **Re15** was 360 μM. According to these values, it was assumed that the ligand had higher selectivity compared to its complex. The absorption peak of **Re15** was at 307 nm, which was due to MLCT. The short Re–N bond length and the long N–S bond length indicate that the **Re15** complex is a good donor. The intense fluorescence displayed by the complex was quenched by coordinating it with Re (Fig. 5).[36]

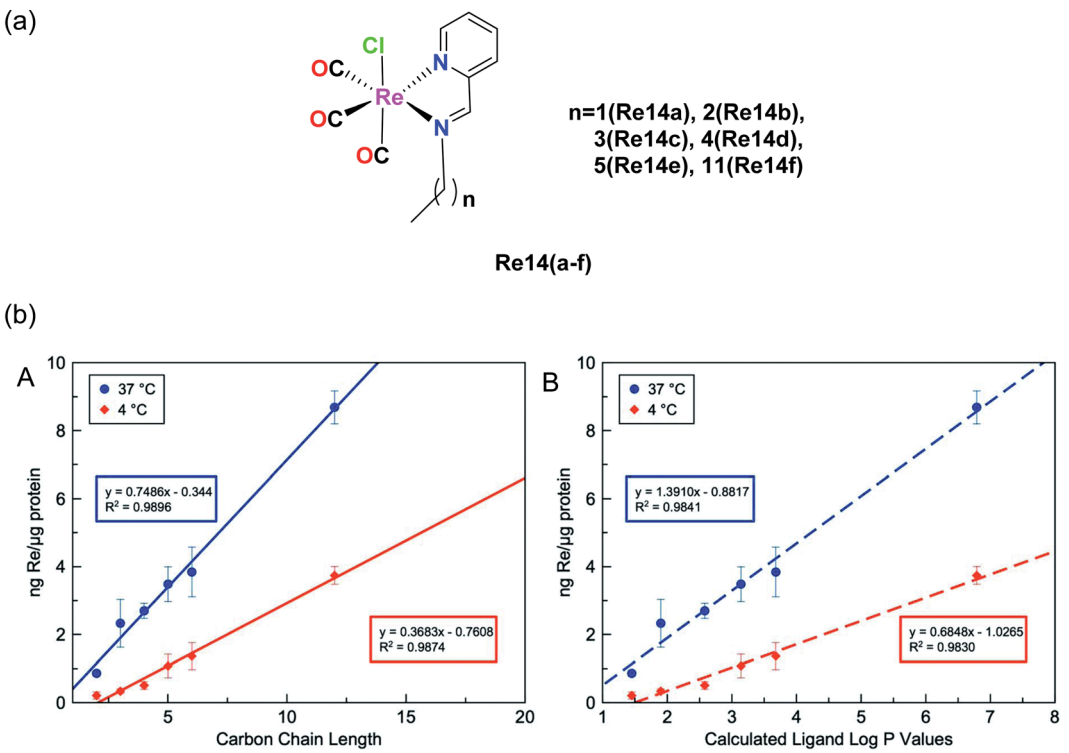

Fig. 4 (a) Structures of Re(I) tricarbonyl complexes bearing pyridyl imine ligands. (b) Cellular uptake of Re-chains after incubation for 3 h at 37 °C (blue) and 4 °C (red) in relation to (A) carbon chain length and (B) calculated log *P* values for the free ligands. The error bars represent the standard deviation from three replicates. [Adapted from ref. 33 with permission from The Royal Society of Chemistry.]

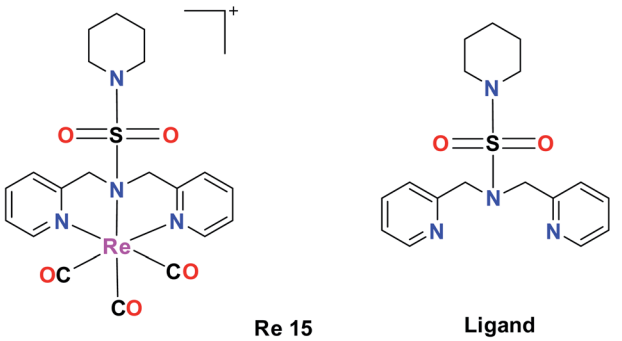

Fig. 5 Structure of Re complex with the formula $[Re(CO)_3(N(SO_2pip)dpa)]^+$ and its ligand.

Nunes *et al.* synthesized benzothiazole Re(I) tricarbonyl complexes, which were stabilized by a cysteamine-based (N, S, and O) chelator containing 2-(4-aminophenyl) benzothiazole pharmacophores [**Re16(a–d)**] (Fig. 6a). MCF-7 and prostate cancer (PC3) cell lines were used to assess the cytotoxic activity of the ligands using the MTT assay. The **Re16(b–d)** complexes exhibited higher cytotoxicity in the MCF and PC3 cell lines. **Re16c** and **Re16d** were the most potent in both cell lines with IC_{50} values of 15.9 μM and 32.1 μM, respectively. They also had an ether-containing linker, and hence were the most active. **Re16a** showed a relatively high IC_{50} value of >50 μM, where the cytotoxicity of these complexes correlated well with their cellular uptake. The highest cytotoxicity was found for **Re16c** in the MCF-7 and PC3 cancer cell lines. Moreover, it was confirmed by fluorescence microscopy that the **Re16c** complex was found

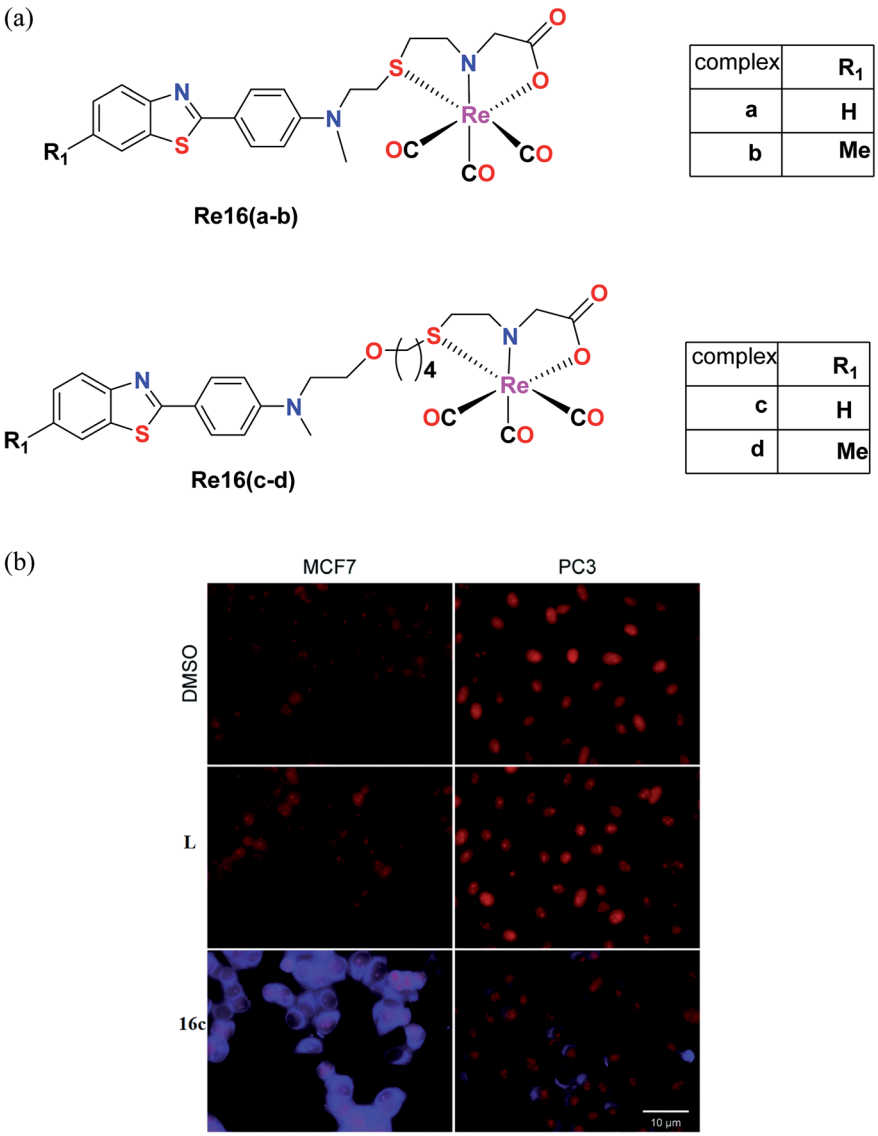

Fig. 6 (a) Structure of Re tricarbonyl complexes with the general formula $ReCO_3(NSO)$. (b) Fluorescence microscopy evaluation of the uptake of L and **Re16c** (blue) in human MCF7 and PC3 cells. Nuclei (red) were stained with propidium iodide. Scale bar: 10 μm. [Adapted from ref. 37 with permission from The Royal Society of Chemistry.]

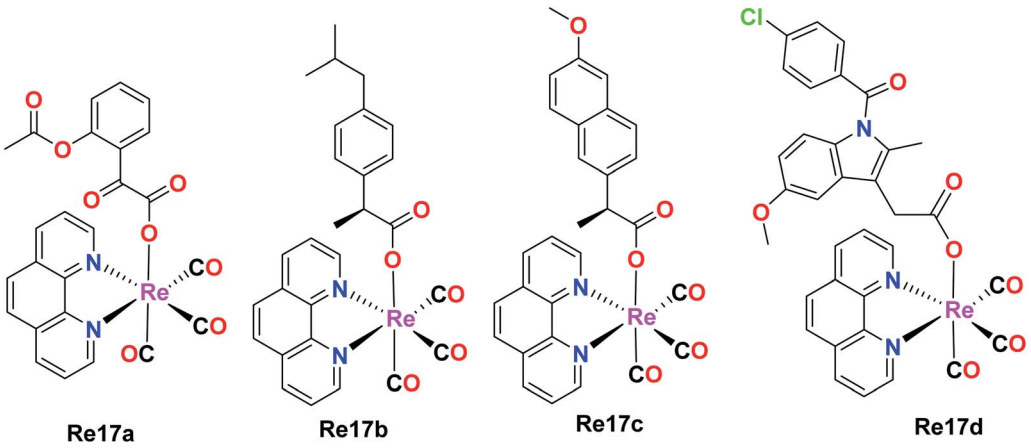

Fig. 7 Structures of fac-[Re(CO)$_3$(phen)(NSAID)] complexes.

to be not only accumulated in the cytosol, but it could also reach the cytoplasm of the MCF-7 and PC3 cell lines.[37]

Luminescent rhenium(I) tricarbonyl complexes

Skiba *et al.* synthesized and reported four fac-[Re(CO)$_3$(phen)(L)] complexes with phen = 1,10-phenanthroline and L = aspirin (**Re17a**), ibuprofen (**Re17b**), naproxen (**Re17c**), indomethacin (**Re17d**). These complexes showed orange phosphorescence from the lowest ^{3}MLCT state and moderate intense luminescence with a broad emission band at 640 nm. **Re17(a–d)** were tested against human cervical epithelioid carcinoma cells (HeLa) and compared to non-tumorigenic mouse murine fibroblast L929 cells for *in vitro* cytotoxicity with the MTT and LDH assay. **Re17(b–d)** were inactive under all conditions with IC_{50} values greater than 150 μM. **Re17a**, which is fac-[Re(CO)$_3$(phen)(aspirin)] (IC_{50} = 36 μM), showed better results compared to other complexes. **Re17(a–d)** were more sensitive to HeLa cells. It exerted two modes of action, *i.e.*, apoptosis induction activity triggered by mitochondrial accumulation and COX-2 inhibitory activity, which is the characteristic property of the aspirin ligand (Fig. 7).[41]

Murphy *et al.* designed Re tricarbonyl complexes with axial nitrogen donor ligands of varying basicity, fac-[Re(CO)$_3$(phen)(L)]$^+$, where phen = 1,10-phenanthroline and L = pyridine (**Re18a**), piperidine (**Re18b**), morpholine (**Re18c**), and thiomorpholine (**Re18d**) and tested against HeLa cells *via* the MTT assay to comprehend their cytotoxicity. **Re18b** (IC_{50} = >164 μM) and **Re3** (IC_{50} = >185 μM) showed very poor cytotoxicity, whereas **Re18d** had modest cytotoxicity (IC_{50} = 36 μM) together with **Re18a** (IC_{50} = 51 μM). The reported rhenium complexes were found to be significantly less active compared to the current clinically approved cisplatin drug (IC_{50} = 6.6 μM) in HeLa cells because of their low intracellular luminesce, suggesting they were poorly taken up by cells. **Re18a** accumulated in the cytosol. The Re complexes were shown to have π–π* inter ligand transitions and lower energy absorbance maximum at 367 nm arising from the excited MLCT (Fig. 8).[44]

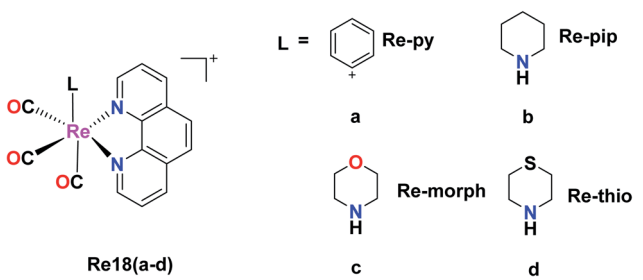

Fig. 8 Structure of fac-[Re(CO)$_3$(phen)(L)]$^+$.

Re–NHC complexes

Simpson *et al.* were the first researchers to report Re–NHC [N-heterocyclic carbene ligands]. **Re61(a–d)** were tested against a variety of pancreatic cancer cell lines (HPFA-II, ASPC-I, and CFPAC) to determine their biological activities. **Re19b** was ineffective at a concentration of 10 μM, while **Re19a**, **Re19c**, and **Re19d** showed complete inhibition. **Re19d** was more active than **Re19(a and b)**, and also effective at higher concentrations in HEK293T cells, indicating its moderate selectivity towards pancreatic cells over healthy cells. The IC_{50} values of the **Re19a**, **Re19b**, and **Re19d** complexes and carboplatin in ASPC-I were 7.9 μM, 6 μM, 4 μM and 6.8 μM, respectively. By observing the IC_{50} values, we can assume that these rhenium compounds are remarkably active towards the tested pancreatic cancer cell lines with similar or slightly higher activity than carboplatin. The anti-cancer activity of these complexes originated from the lability of their ancillary ligand. **Re19a** and **Re19d** did not show any morphological changes related to apoptosis, but they showed the existence of multinucleated cells, suggesting cell arrest at the G2/M phase. These complexes were able to inhibit the phosphorylation of Aurora-A in the pancreatic cancer cell lines. **Re19d** inhibited anchorage-independent growth. The above-mentioned Re complexes were the first rhenium NHC complexes exhibiting anticancer activities. The future work on these complexes would be aimed at investigating their *in vitro* and *in vivo* cytotoxic properties, and also assessing their *in vivo* antitumor activity (Fig. 9).[45]

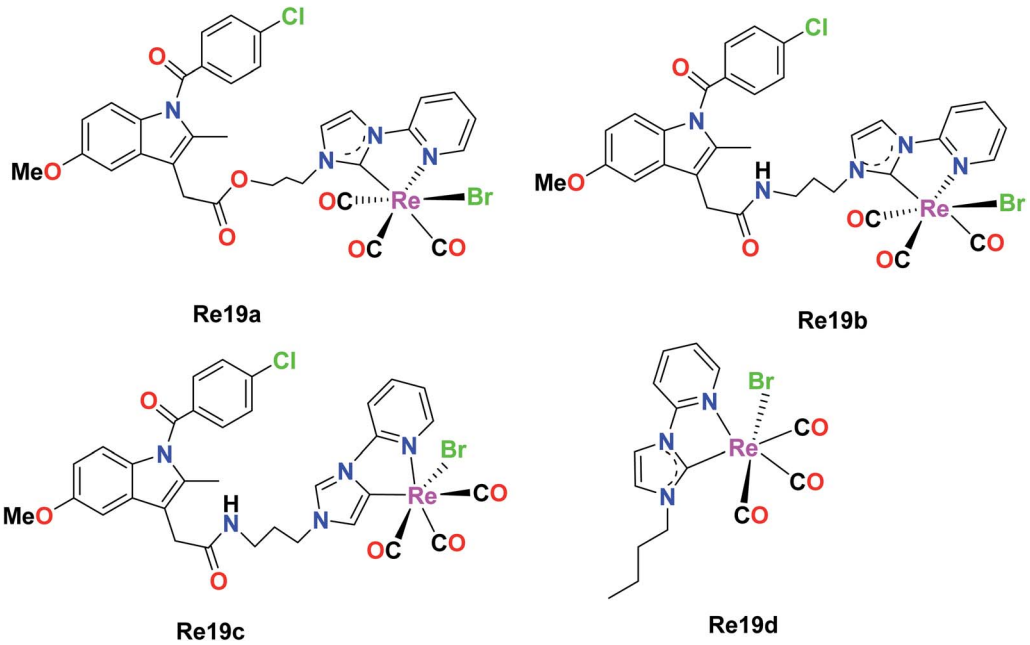

Fig. 9 Structure of $[Re(CO)_3(NHC)]$ complexes.

Phosphorescent rhenium(I) tricarbonyl complexes

Liang He *et al.* synthesized **Re20a** and **Re20b** bearing β carboline derivatives (Fig. 10a). These complexes showed intense absorption bands in the UV region at 230–300 nm, which are attributed to π–π* transitions, and lower energy broad peaks corresponding to ligand transfer ^{1}MLCT. They were tested against different cell lines such as A549, A549R (cisplatin-resistant cells), HeLa cells, MCF-7 and human lung fibroblasts (HLF) *in vitro* to determine their cytotoxic activity. These complexes showed better cytotoxic results compared to cisplatin. **Re20b** was 4 times more potent than cisplatin against A549 cells and 5.8 times higher cytotoxicity against lung cancer A549 cells compared to non-cancerous HLF cells. They also exhibited higher activity against A549R cells, with greater anticancer efficacy than cisplatin, revealing their ability to overcome cisplatin resistance. The complexes showed pH-dependent phosphorescence, targeting lysosomes. **Re20(a and b)** were less cytotoxic to HLF cells, indicating certain selectivity. **Re20b** had low systemic toxicity and could inhibit tumor cell proliferation. The reported Re complexes showed pH-dependent phosphorescence. The authors investigated the lysosomal effect of **Re20b** with the help of acridine orange (AO) staining. After comparison with the control group, they found that the cellular red AO fluorescence intensity decreased after treatment with **Re20b**. This observation revealed the disruption of the lysosome integrity (Fig. 10b). **Re20b** also induced caspase-independent apoptosis, causing lysosomal dysfunction, and thus impaired the lysosomal enzymatic activity. These complexes could specifically image the acidic lysosomes. The reported **Re20(a and b)** tricarbonyl appeared to induce autophagy-mediated cell death, which was the first report on this function.[55]

Yang *et al.* synthesized eight organometallic rhenium(I) phosphorescent complexes, $[Re(CO)_3(N\text{–}N)L]PF_6$ {N–N = 1,10 phenanthroline (phen) or 4,7-diphenyl-1,10 phenanthroline (DIP)}. These complexes (Fig. 11a) were suitable for targeting the mitochondria, and simultaneously induced the tracking the therapeutic effect on the mitochondria of human A549 cells under study. The *in vitro* cytotoxicity of the synthesized Re complexes were tested against various cell lines, namely, HeLa, human pulmonary carcinoma, A549, human lung carcinoma, A549R, cisplatin-resistant cell line, and LO2, human normal liver cell line. The cytotoxicity was determined *via* the MTT assay. Their studies showed that the **Re21(e–h)** complexes with DIP ligand had greater cytotoxicity than the **Re21(a–d)** complexes with the phen ligand, which showed moderate to non-cytotoxicity. The IC_{50} values of the **Re21(a–d)** complexes were in the range of 0.52 μM to 22.4 μM and were also higher compared to the IC_{50} values of cisplatin for all the tested cell lines. Interestingly, the toxicity of the **Re21(e–h)** complexes was lower towards normal cells, whereas they showed high selectivity towards the cancer cells. Among the tested cell lines, the cytotoxicity was high towards the A549R cell line, which also indicated that these complexes have the ability to overcome the cisplatin resistance in this cell line. In particular, the **Re21g** complex $[Re(CO)_3(DIP)(py\text{-}3\text{–}CH_2Cl)]$ showed remarkable cytotoxicity against cancer cells. The potency of this complex to kill the A549, HeLa and cisplatin-resistant A549R cells was 7-fold, 17-fold, and 87-fold potent than the cisplatin drug, respectively. **Re21g** was also seen to be more selective towards the A549 and HeLa cells by 6-fold and 36-fold, respectively, over the normal cells. By further studies, it was concluded that the remarkable cytotoxicity and selectivity of **Re21c** were partially due to its high retention time immobilization capacity in mitochondria. Also, the excellent phosphorescence of the **Re21g** and **Re21b**

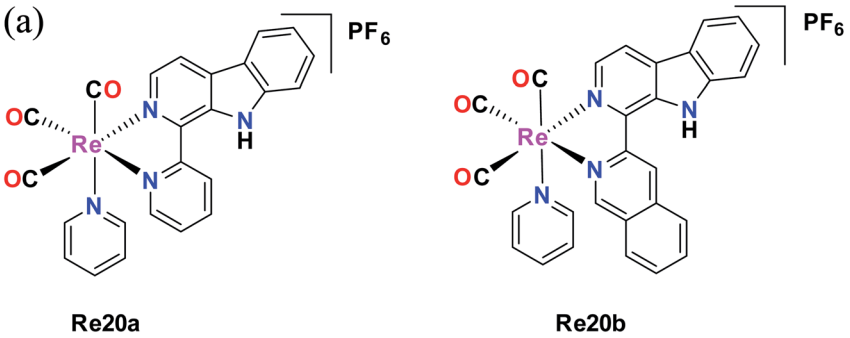

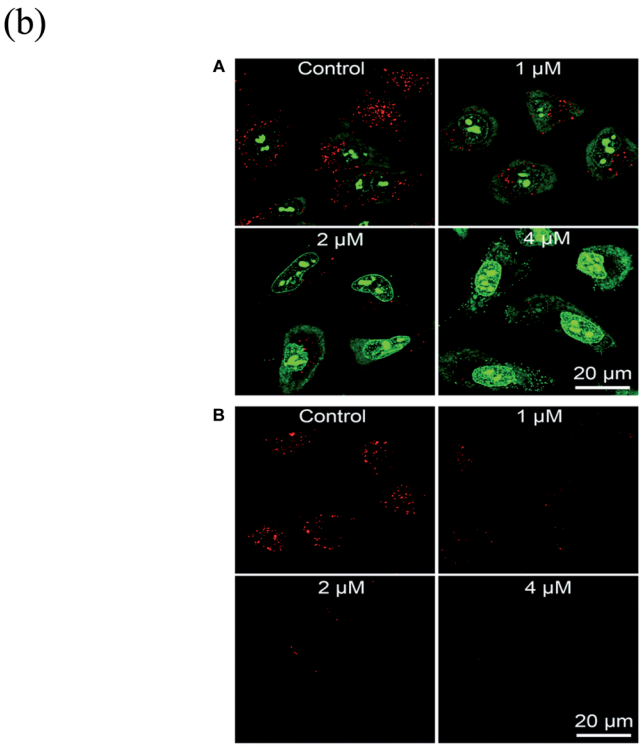

Fig. 10 (a) Structure of Re(I) tricarbonyl complexes with the general formula $[Re(CO)_3(py)(L)](PF)_6$. (b) (A) Detection of lysosomal disruption upon **20b** treatment in A549 cells by AO staining. (B) Observation of cathepsin B activity upon **20b** treatment in A549 cells using the fluorogenic substrate Magic Red MR-(RR)2. [Adapted from ref. 55 with permission from The Royal Society of Chemistry.]

complexes could be used for tracking the Re(I)-induced mitochondria morphological changes in real-time. The rhenium complexes could induce cellular ATP depletion, mitochondrial respiration inhibition, reactive oxygen species elevation (ROS), mitochondrial damage, and caspase-dependent apoptosis.[57]

Rhenium(I) tricarbonyl Cp* complexes

Imine-functionalized cyrhetrenyl aldehyde-derivatized rhenium complexes with the formula $[(\eta^5\text{-}C_5H_4CHO)Re(CO)_2PR_3]$, where R = methyl (Me, **Re22a**), phenyl (Ph, **Re22b**) and cyclohexyl (Cy, **Re22c**), were synthesized by Siegmund *et al.* The cytotoxicity of these **Re22(a–c)** complexes was studied on human cancer cell lines PT-45 and HT-29 by the MTT assay. The **Re22a** complex with the triphenyl phosphine ligand exhibited striking cytotoxic activity on both the cancer cell lines. The PT-45 cell line showed an IC_{50} value of 11.5 μM and was seen to be more sensitive to the **Re22b** complex compared to the HT-29 cell line. In contrast, the HT-29 cell line was more sensitive and more active than the PT-45 cell line on direct comparison with the cisplatin drug. The **Re22c** complex showed no cytotoxic activity on both cell lines. According to the results, the presence of aromatic rings in the **Re22b** complex increased the lipophilicity, which helped to ease the cellular uptake, and thereby increased the biological activity of the **Re22b** complex. Thus, alterations in the phosphine ligand substituents can lead to promising and enhanced biological activity in organometallic rhenium drugs as potential anticancer agents (Fig. 12).[56]

Fluorescent Re(I) tricarbonyl complexes

The fluorescent Re(I) complexes $[Re(CO)_3(L)]BF_4$ and **L1** were also synthesized and tested for their anticancer, cell imaging and photophysical properties by Jones *et al.*, where 1,9-dicarboximide

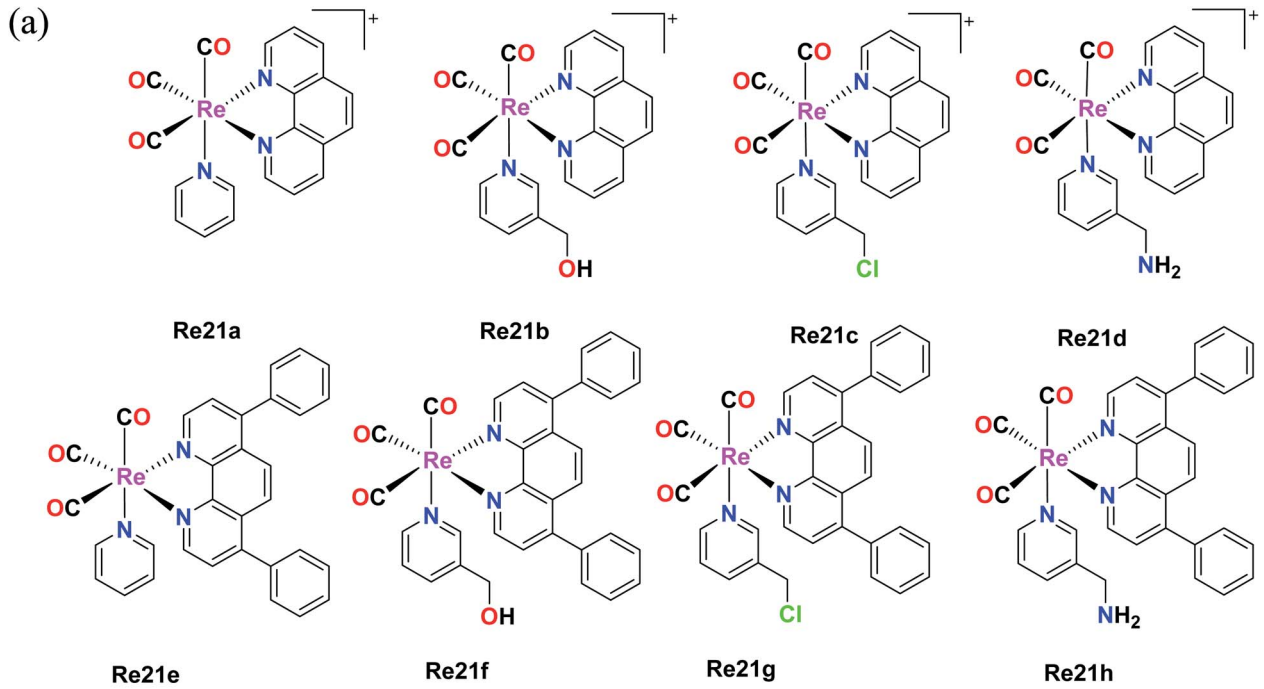

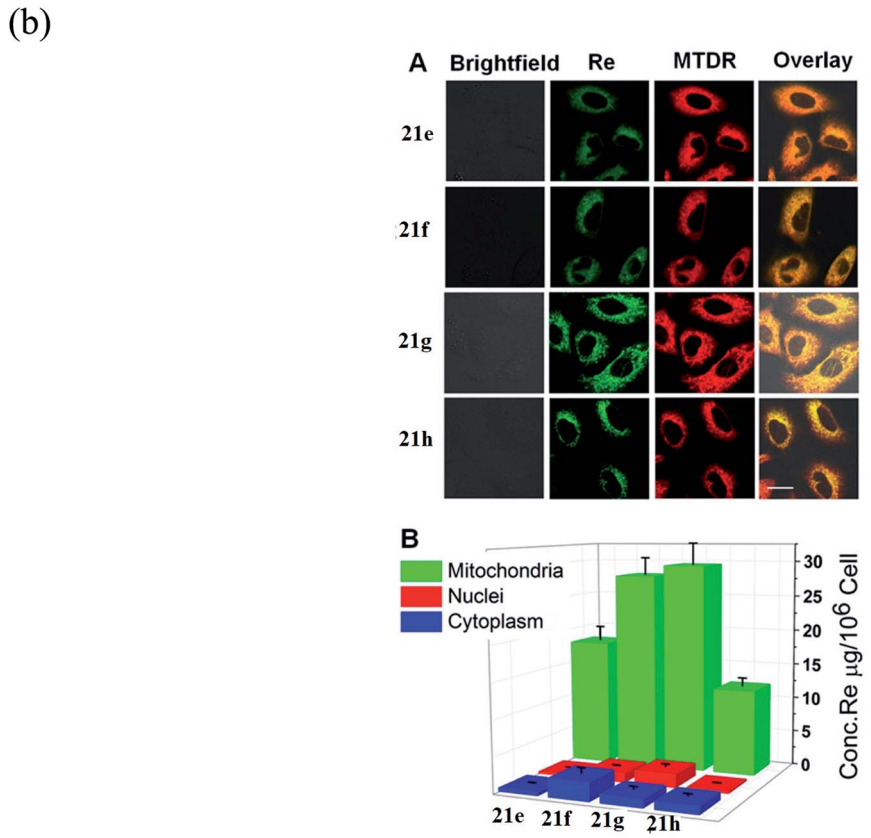

Fig. 11 (a) Chemical structures of Re(I) complexes with the general formula $[Re(CO)_3(N{-}N)L](PF_6)$. (b) (A) Intercellular colocalization of **21e–21h** with MTDR imaged by CLSM. A549 cells were incubated with 20 μM and at 20 min, and then stained with MTDR (150 nM, 30 min) at 37 °C (**1b–4b**, $\lambda_{ex} = 405$ nm and $\lambda_{em} = 550 \pm 30$ nm; MTDR, $\lambda_{ex} = 633$ nm and $\lambda_{em} = 655 \pm 20$ nm). (B) Distribution of complexes **21e–21h** (20 μM, 1 h) in various organelles of A549 cells measured by ICP-MS. [Adapted from ref. 57 with permission from the American Chemical Society.]

was exploited as the fluorophore in this compound. The cytotoxicity of the **23L1** and **23L2** ligands and the two **Re23(a and b)** complexes was investigated against the A549 (lung carcinoma), LOVO (colon adenocarcinoma), PC3 (prostate adenocarcinoma) and MCF7 (breast adenocarcinoma) cells by the MTT assay. Among the ligands, **23L2** showed the least toxicity, unlike **23L1** which was a highly toxic compound. The high toxicity of the **23L1** ligand, especially towards MCF7 cells can be attributed to its high lipophilicity. The **23L2** ligand showed a greater complexation effect towards the Re(I) metal complex. The cytotoxic activity and the cellular imaging capability of the complexes could be due to the ligand structures and the lipophilicity of the fluorophores. Also, the intracellular localization of the fluorophores was dependent on their structures. The **23L1** and **23L2** ligands and the resultant complexes were fluorescent in the visible region (490 nm). The mode of action of these complexes and the investigation of toxicity towards non-cancerous cell lines will be helpful for their future application (Fig. 13).[58]

Organorhenium complexes with the general formula $XRe(CO)_3Z$ (X = α-diimines and Z = *p*-toluene sulphonate (**Re24a**), picolinate (**Re24b**), nicotinate (**Re24c**), 1-naphthalene sulfonate (**Re24d**), ibuprofenate (**Re24e**), 2-naphthalene sulfonate, aspirinate, naproxenate, flufenamate, mefenamate, tolfenamate, and *N*-acetyl tryptophanate) were synthesized and evaluated for their cytotoxicity against the hormone-dependent MCF-7 and the hormone-independent triple-negative MDA-MB-231 breast cancer cell line using the Alamar Blue assay by Wilder *et al.* The most active cancer cell lines for the organorhenium complexes were MCF-7 and MDA-MB-231. The IC_{50} of **Re24a**, **Re24b**, **Re24c**, **Re24d**, and **Re24e** on these cell lines was in the range of 0.25 μM–1.00 μM. The IC_{50} values of **Re24a** and **Re24c** were 0.2 μM and 0.5 μM on MDA-MB-231, respectively. It was also found that the non-steroidal anti-inflammatory drugs (NSAIDs) of the organorhenium complexes were inactive against breast cancer cells. The increase in the anticancer activity of the organorhenium complexes can be attributed to the increase in lipophilicity of the compounds. The complexes were highly competent to intercalate DNA. The complexes were very selective towards cancer cells and showed very low activity towards normal cells. Thus, these complexes have potential as efficient anticancer drugs (Fig. 14).[59]

Delasoie *et al.* characterized and reported Re(I) tricarbonyl complexes with the formula fac-[Re(I)$(CO)_3$]N, where N is ([2,2′-bipyridin]-6-ylmethyl). For cytotoxicity, these complexes (Fig. 15a) were verified against the cell lines of A549, HCT-116 (colorectal carcinoma cells), MIAPaCa-2 (pancreatic carcinoma cells) and MRC-5. **Re25(a–d)** showed higher anti-proliferative activity than the **Re25(e–h)** complexes. **Re25(a–d)** exhibited the highest potency against HCT cells and MIAPaCa-2 cells with IC_{50} values in the range of 5–10 μM. **Re25c** was the most active compound on all the tested cell lines except HCT116. **Re25a** and **Re25d** showed moderate selectivity between healthy and cancer cells, and also showed greater anti-proliferative activity. The IC_{50} values of complexes **Re25(a–h)** in HeLa cells followed the order of 1.2 μM, 0.7 μM, 1.2 μM, 1.0 μM, 1.3 μM, 1.5 μM, 1.2 μM, and 1.3 μM. The *in vivo* toxicity of these complexes was investigate using zebrafish. The toxicity followed the order of **Re25c** = **Re25b** ≫ **Re25a** > **Re25d**. Complex **Re25c** and **Re25d** had

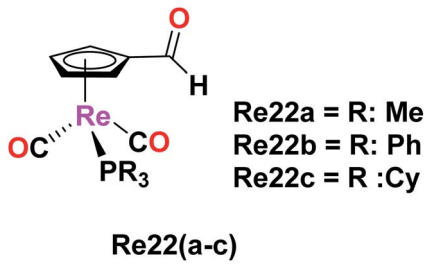

Fig. 12 Structure of Re complex with the formula $[(\eta^5C_5H_4CHO)Re(CO)_2PR_3]$.

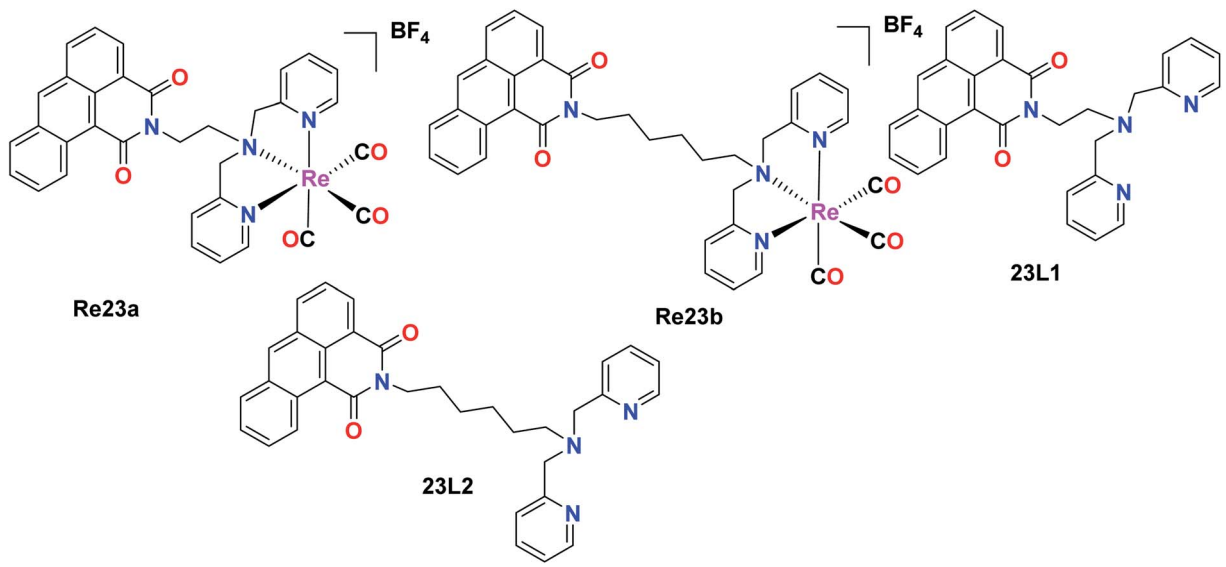

Fig. 13 Structure of Re complexes with the formula $[Re(CO)_3(L)]BF_4$.

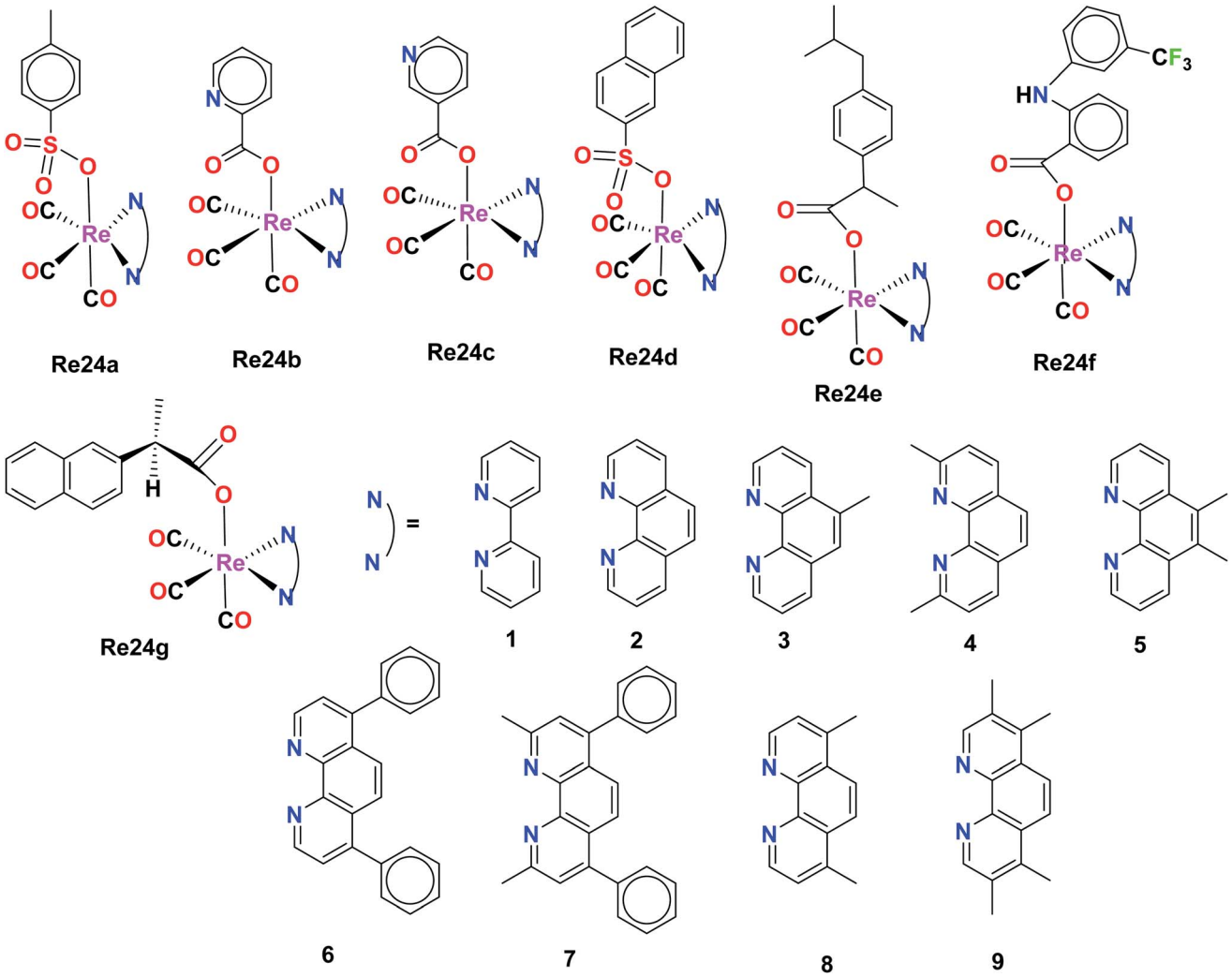

Fig. 14 Structure of the Re complexes with the formula $XRe(CO)_3Z$.

a toxic effect of >25 μM. **Re25a** and **Re25b** did not cause any cardiac dysfunctions. **Re25a** and **Re25d** were highly effective in inhibiting angiogenesis and also reduced the tumor mass in treated xenografts by 38%. These Re(I) tricarbonyl complexes were treated against colorectal carcinoma *in vivo* to evaluate their anticancer activity. **Re25a** and **Re25d** exhibited colorectal tumor growth and cancer cell dissemination. These complexes were effective even at a concentration 8 times less than the respective *in vitro* IC_{50}. **Re25a** exhibited 2.3 times greater anticancer potency than **Re25b**. The lipophilicity of the complexes followed the order of **Re25i** < **Re25b** < **Re25a** < **Re25c** < **Re25d** < **Re25e**. These complexes exhibited weak fluorescence with a maximum emission wavelength at 624 nm and 606 nm. The internalization of these complexes may occur *via* an energy-dependent process. **Re25a** and **Re25d** were distributed in the cytoplasm of HCT-116 cells (Fig. 15b) and the complexes were partially localized in the lysosomes, acting by altering cellular processes possibly by alkylation *via* one or several key proteins. These complexes possessed triple anticancer, anti-angiogenic (displayed 349 times higher activity than the clinical drug sunitinib malate) and antimetastatic activity. The complexes had a large therapeutic window (200 μM–250 μM), inducing no toxicity issues in clinical anticancer drugs. Their future work is aimed at the anti-tumor efficacy and therapeutic potential of molecules on primary tumor cells together with their mechanism of action.[60]

Four rhenium(I) diimine complexes with the general formula fac-$[Re(CO)_3(\alpha\text{-diimine})\{4\text{-}C_{11}\text{-py}\}]CF_3SO_3$, where (α-diimine = 2,2-bipyridine (**Re26a**), 4,4-ditert-butyl-2,2-bipyridine (**Re26b**), 4,4-dinonyl-2,2-bipyridine (**Re26c**), and $4\text{-}C_{11}$py = 4-undecylpyridine) and fac-$[Re(CO)_3(\alpha\text{-diimine betaine})(4\text{-Etpy})]CF_3SO_3$ (**Re26d**), where (α-diimine = 2,2-bipyridine, 4-Etpy = 4-ethyl pyridine) were synthesised by G. Balakrishnan *et al.* The **Re26(a–c)** complexes possessed long alkyl chains. The biological activities of these complexes were studied and reported in this paper. The DNA binding studies showed that the **Re26(a–d)** complexes were very competent to bind with calf-thymus DNA (ct-DNA). The moderate binding of the complexes with the ct-DNA was facilitated by the presence of hydrophobic alkyl groups on the ligands bipyridine (bpy) and pyridine (py). The

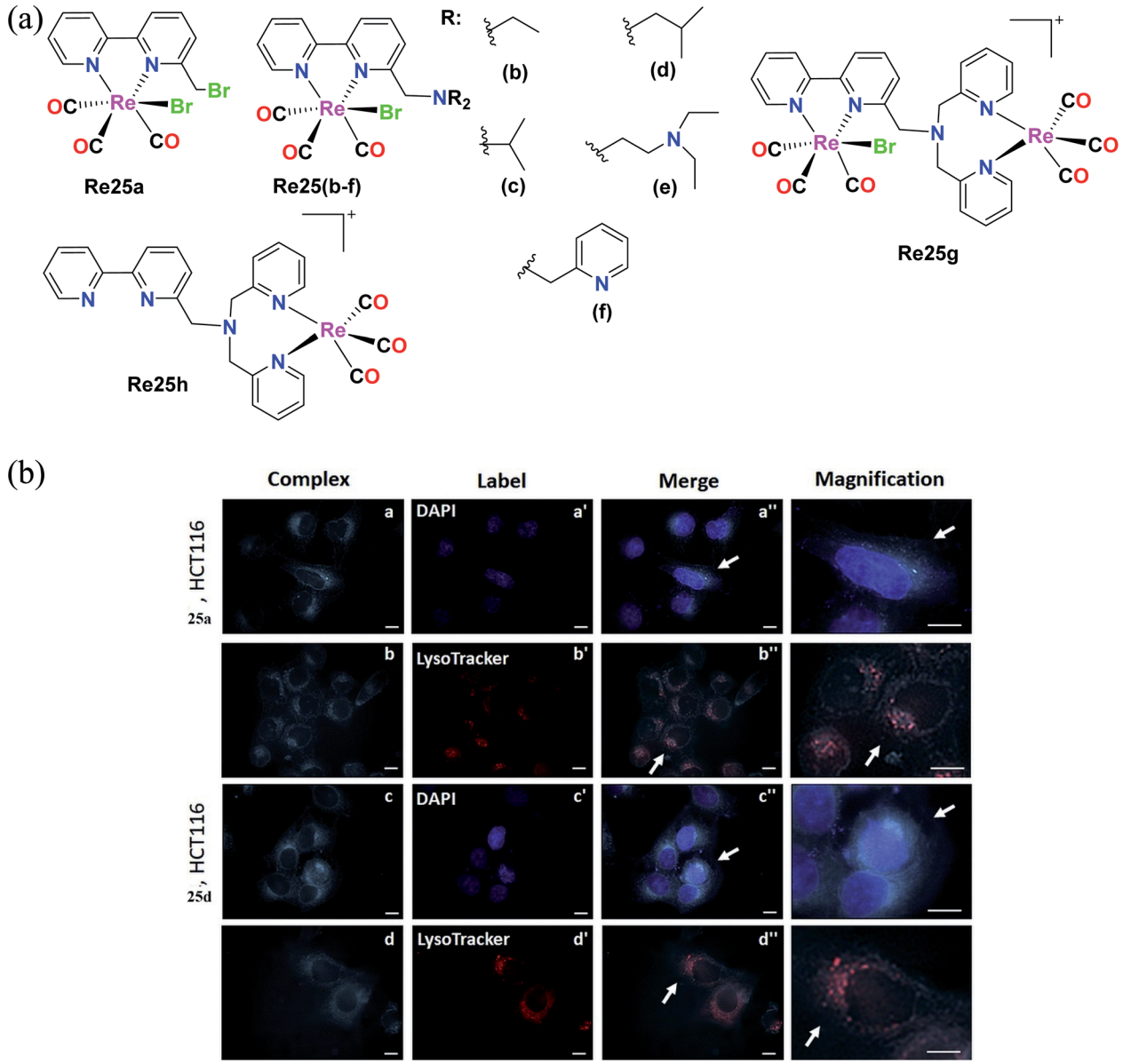

Fig. 15 (a) Structure of Re(I) complexes with the formula fac-[Re(I)(CO)$_3$]N. (b) Fluorescent microscope images of HCT-116 cells treated with **25a** and **25d** (5 μM, 30 min, 37 °C/5% CO_2). Intracellular distribution of complex **25a** (a and b) and complex **25d** (c and d), as well as of DAPI-labelled nuclei (a′ and c′) and LysoTracker-labelled lysosomes (b′ and d′). Co-localization of the applied complexes with DAPI or LysoTracker dye is shown on images a″–d″. Arrows indicate magnified cells in the last column. Magnifications ×100 was used. Scale bars = 10 μm. [Adapted from ref. 60 with permission from Elsevier.]

complexes were investigated for their cytotoxic activity on Raji (B cell lymphoma) and Jurkat (T cell lymphoma) cell lines by the MTT assay. The resulting IC_{50} values were compared with normal human peripheral blood mononuclear cells (PBMCs). The cytotoxicity of all the synthesized Re(I) complexes was higher than the PBMCs. The order of the cytotoxicity of the **Re26(a–c)** complexes against the tested cell lines followed the order of **Re26c** > **Re26b** > **Re26a**. The **Re26c** complex could be used as a good fluorescent probe for cellular imaging and diagnosis of disease in pathological conditions. The **Re26(a–c)** complexes also showed antibacterial activity. The ability of these complexes to bind to DNA was observed to follow the order of **Re26c** > **Re26b** > **Re26a** > **Re26d** (Fig. 16).[61]

Mitochondria-targeting Re(I) tricarbonyl complexes

Garcia *et al.* reported the preparation of three Re(I) tricarbonyl complexes [ReCl(CO)$_3$(H_2AcPh)] (**Re27a**), [ReCl(CO)$_3$(H_2-AcpClPh)] (**Re27b**) and [ReCl(CO)$_3$(H_2AcpNO$_2$Ph)] (**Re27c**). These complexes were treated with non-small lung cancer (NSCI-H460) and human umbilical vein endothelial cells (HUVECs). **Re27c** was the most cytotoxic (IC_{50} of 16.5 μM). These complexes with hydrazones induced apoptosis, reduced the production of ROS and mitochondrial damage on NSCI-H460 cells. The IC_{50} values of **Re27(a–c)** on NCi-H460 were 58.1 μM, 20.5 μM, and 16.0 μM, respectively. **Re27b** and **Re27c** did not show any selectivity but the *in vitro* cell viability study on

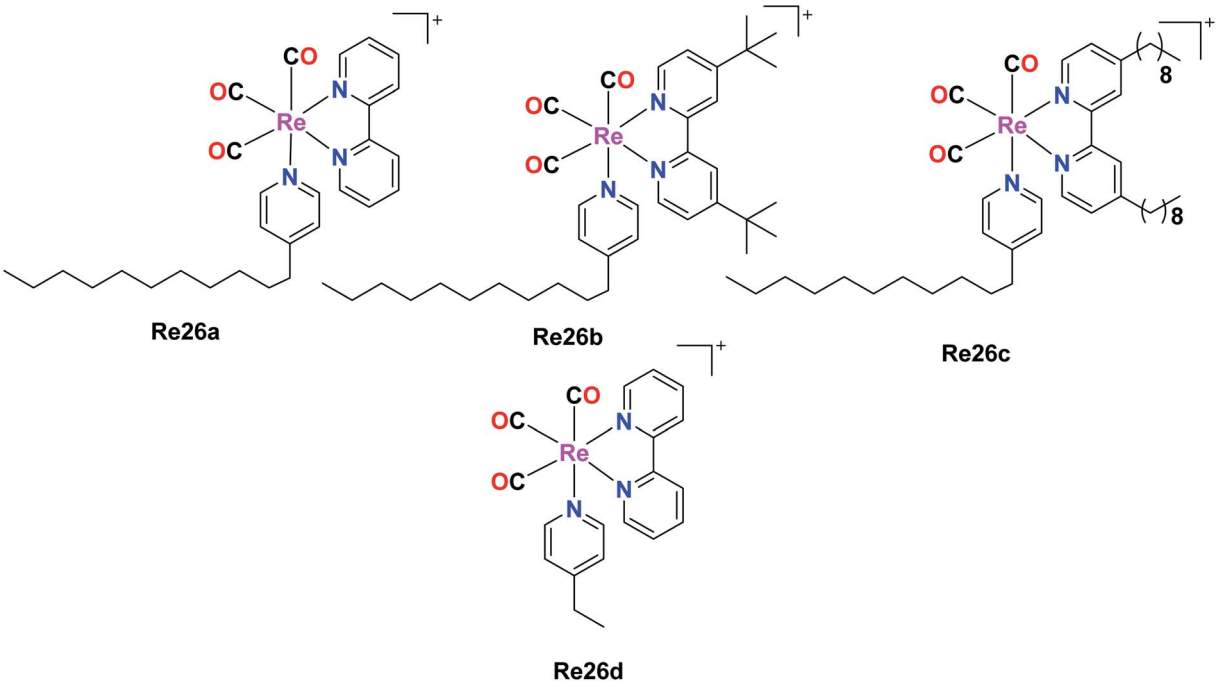

Fig. 16 Structure of the Re complexes with the formula fac-[Re(CO)$_3$(α-diimine){4-C$_{11}$-py}]CF$_3$SO$_3$.

HUEVCs in the presence of the complexes suggested the inhibition of endothelial cell proliferation. Further work was carried on the effect of complexes **Re27b** and **Re27c** on angiogenesis, which caused apoptosis *via* both mitochondria-dependent and mitochondria-independent pathways (Fig. 17).[62]

Wilson *et al.* synthesized Re(I) tricarbonyl complexes **Re28a**, **Re28b** and **Re28c**. These compounds revealed very good cytotoxicity results (IC$_{50}$ > 10 μM), which were tested against A2780, A2780CP70, HEK293 (kidney cells), respectively. Among them, **Re28c** was the most potent in the ovarian cancer cell lines and most active in the HeLa cell lines, producing very low micromolar IC$_{50}$ values in HEK293 cells. **Re28c** also gave larger HS (Hill slope) values of around 10–15 across the A270 and A2780CP70 cell lines. The IC$_{50}$ values of **Re28a**, **Re28b** and **Re28c** in A2780 were 5.1 μM, 4.3 μM and 3.2 μM, respectively. The *in vitro* therapeutics of these complexes was higher than that of cisplatin. These complexes shared a strong electron-donating diethylamino substituent of aniline, indicating the important structural features, which resulted in enhanced cytotoxic properties. **Re28(a–c)** also contained substituents at the *para* position of picolinaldehyde. **Re28c** did not induce cell death by ROS, rather it instigated plasma membrane rupture, and thereby could be accumulated in mitochondria (Fig. 18).[63]

Mao *et al.* reported an Re(I) tricarbonyl complex with the formula [Re(DIP)(CO)$_3$(L)](PF$_6$) (**Re29**) (Fig. 19a), where L = (N1-hydroxy-N8-(pyridine-4-ylmethyl)octanediamide), a 4-(aminomethyl)pyridine (**SAHA**). The cytotoxicity of this rhenium complex was evaluated *via* the MTT assay against HeLa nuclear extract (HDACs) and human recombinant cells (HDAC7), A549 and LO2. The **Re29** (IC$_{50}$ = 7.5 μM) complex showed much better results compared to its ligand and cisplatin against all the cell lines tested. **Re29** was 2.5-fold more potent than **SAHA** in HeLa cells and 6.2-fold higher anticancer efficacy than cisplatin, killing A549R cells, demonstrating that this complex could overcome cisplatin resistance. The **Re29** complex also exhibited selectivity towards cancer cells over noncancerous cell, indicating nearly 7 times lower cytotoxicity against LO2 and HePG2 cells. ROS played a vital role in the induced cytotoxicity of **Re29**. **Re29** displayed a high energy inter ligand π–π* and low energy MLCT. This complex could be localized in the mitochondria and inhibit the activities of total HDACs and HDAC7 isoform potently. The subcellular localization of the complex

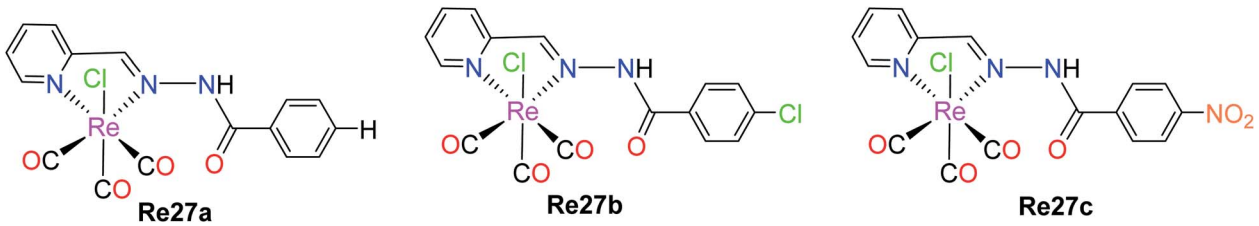

Fig. 17 Structure of Re(I) tricarbonyl complexes with the formula [ReCl(CO)$_3$(XAcPh)].

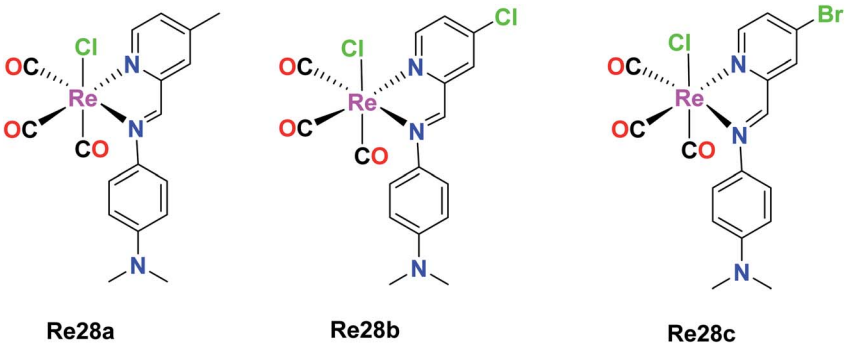

Fig. 18 Structures of Re(I) tricarbonyl complexes having diimine ligands.

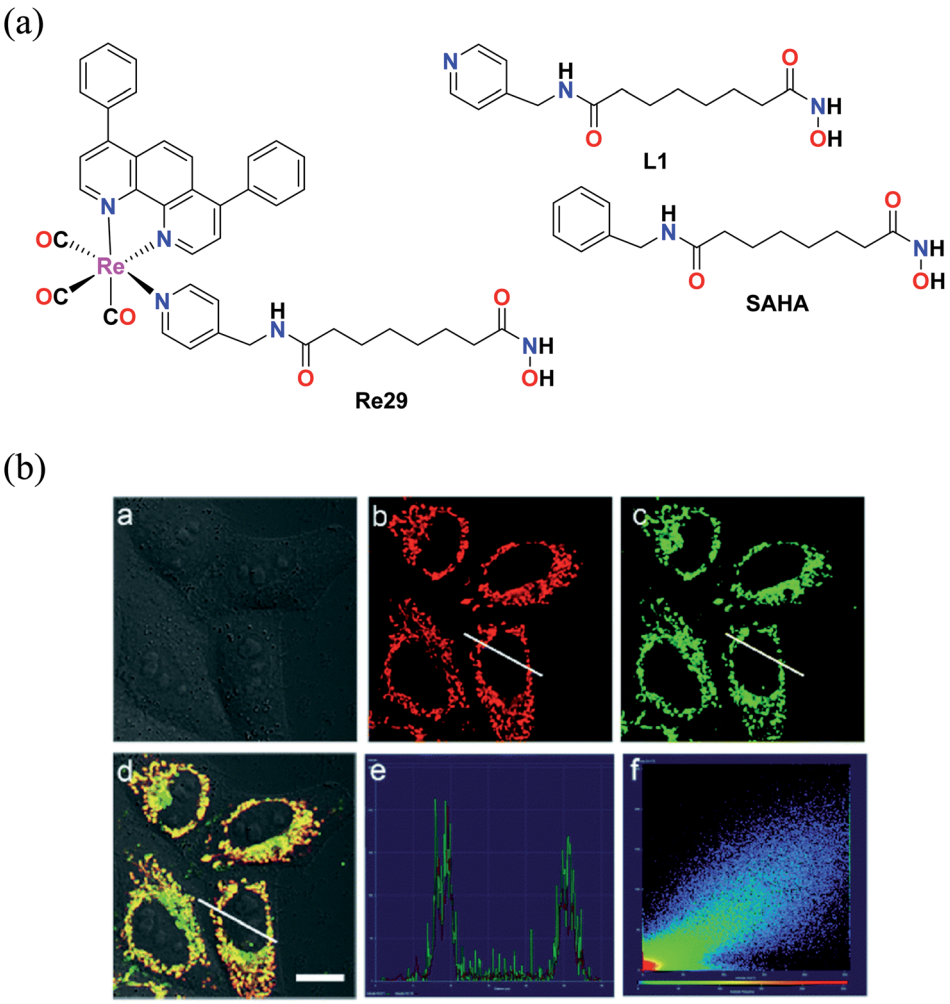

Fig. 19 (a) Structure of Re(I) complexes with the formula $[Re(DIP)(CO)_3(L)](PF_6)$. (b) Confocal microscopy images of HeLa cells co-labelled with **Re29** and MTDR. (a) Bright field. (b) MTDR (100 nM, 0.5 h). (c) **Re29** (20 μM, 2 h). (d) Merged image of (a–c). (e) Intensity profile of regions of interest (ROIs) across HeLa cells. (f) Correlation plot of MTDR and **Re29** intensities. Scale bar: 20 μm. [Adapted from ref. 64 with permission from The Royal Society of Chemistry.]

was investigated by Mito Tracker Deep Red FM (MTDR) (Fig. 19b). The mitochondrial staining of **Re29** was found to exhibit a high Pearson's coefficient value of 0.90. Very low colocalization of this complex was found with LysoTracker Deep Red FM (LTDR). **Re29** was seen to induce caspase-independent parapoptosis through mitochondrial events, which include mitochondrial membrane permeabilization and generation of reactive oxygen species. The complex also affected the nuclear membrane.[64]

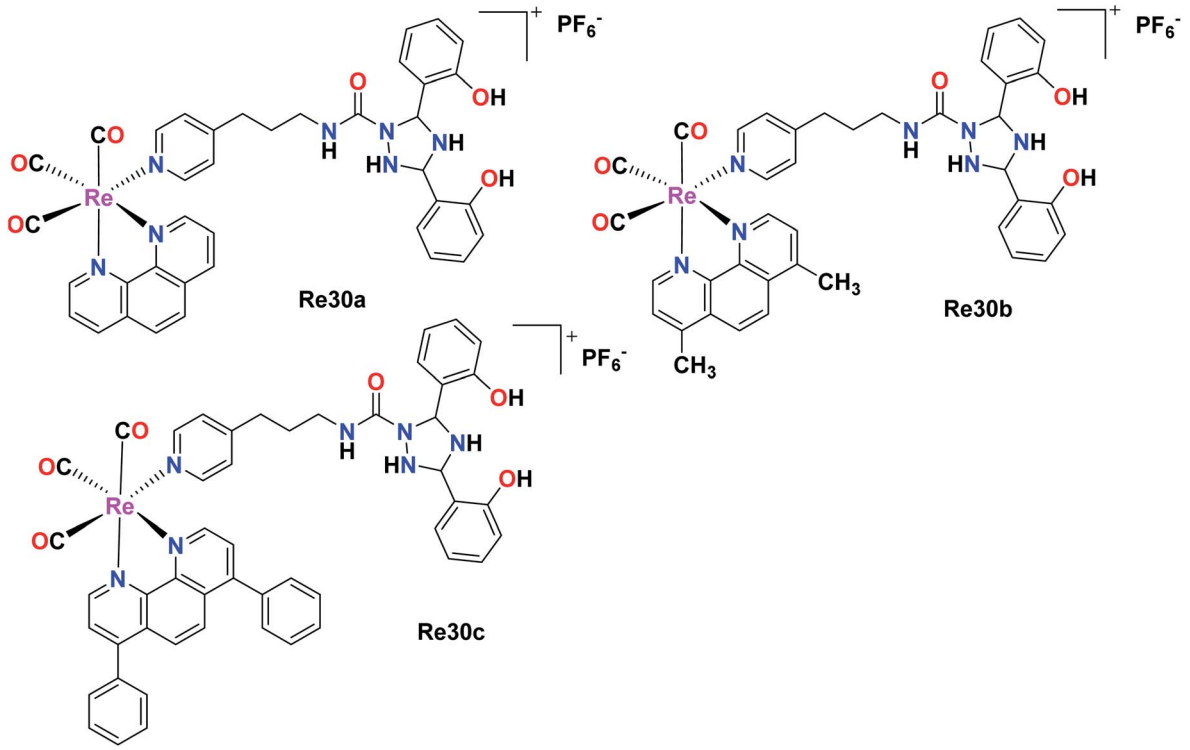

Fig. 20 Structures of Re tricarbonyl complexes.

In this case, Hao *et al.* also synthesised Re(I) complexes, **DFX–Re30a–DFX–Re30c**, which targeted the mitochondria of cancer cells, where DFX represents for deferasirox, an iron-based chelating ligand. Among the 3 complexes and their corresponding control compounds **Re30a–Re30c**, the **DFX–Re30c** complex displayed impressive and selective cytotoxicity against MDA-MB-231 (TNBC) cells. The IC_{50} value was determined to be 0.4 μM, which is 100-fold higher than the cytotoxicity of the platinum-based drug cisplatin. However, the **DFX–Re30c** compound did not show effective cytotoxicity against MCF-7 (breast cancer) and MCF-10A (normal mammary epithelial) cells. Its cytotoxicity (IC_{50}) was 32-fold and 46-fold higher in MCF-7 and MCF-10A cells, respectively, indicating its high activity against TNBC cells. **DFX–Re30c** is indeed the most active rhenium complex reported to date in TNBC cells (Fig. 20).[65]

Konig *et al.* synthesised and reported a phenanthridine-containing $Re(CO)_3$(**Re31**) complex. The *in vivo* anti-proliferative activity of these complexes was evaluated against the human Burkitt lymphoma cell line, exposing very promising anti proliferative activity at low molecular concentrations. The **Re31** complex was selective with a greater impact on malignant cells. **Re31** could overcome the acquired resistance based on *p*-glycoprotein overexpression. **Re31** was localized in the mitochondria, and thus caused a change in mitochondrial potential at lower concentrations. It also invoked the extrinsic and intrinsic apoptotic pathways, providing an extra option for therapeutic applications in drug-resistant cell lines. **Re31** was the first reported phenanthridine-containing Re complex and also helped to induce multiple apoptotic pathways, which can be successfully exploited in chemotherapy (Fig. 21 and 22).[66]

Lysosome-targeting Re(I) tricarbonyl complexes

Knopf *et al.* also reported the preparation of **Re32** {fac-$[Re(CO)_3$(2,9-dimethyl-1,10-phenanthroline)$(OH_2)]$}, and its cellular uptake was measured in A2780 and cisplatin-resistant A2780CP70 ovarian cancer cells. Their studies implied that Re was found in the nuclei but a larger amount of it was found in the mitochondria, signifying the localization of complex in the organelles. **Re32** also induced cytoplasmic vacuolization, localizing primarily in the lysosomes, and also inhibited tumor growth (*in vivo*). The pK_a value of **Re32** was found to be 8.3, where this high pK_a may be due to the increased electron donation by the diamine ligand. The enhanced luminescence intensity of **Re32** was observed at a lower pH. **Re32** was highly dependent on the pH and coordination environment. Re(1) was also minimally

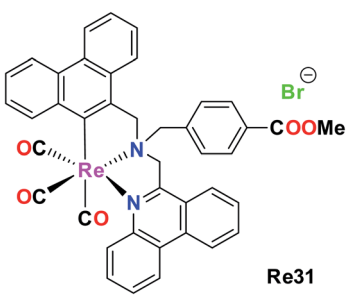

Fig. 21 Structure of organometallic Re complex with the general formula fac-$[Re(CO)_3$(bis(6-phenanthridinyl-methyl)amino)acetic acid methyl ester].

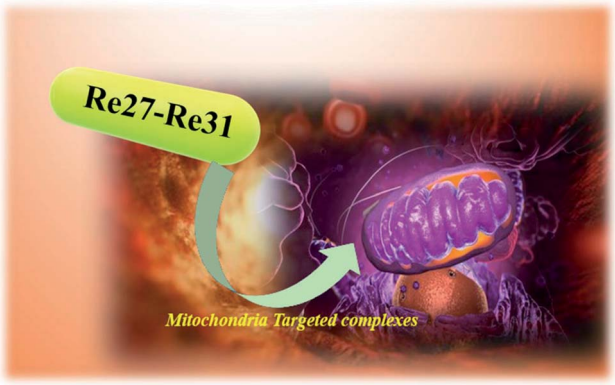

Fig. 22 General pictorial representation of mitochondria-targeting complexes.

toxic throughout the treatment. Further work was carried to explore the biological mechanism of the **Re32** complex (Fig. 23).[67]

Re(I) diselenoether complex

The combined cytotoxic effect of the Re(I) diselenoether (**Re33**), which is a tricarbonyl complex chelating with a diselenoether ligand, was studied by Collery *et al.* This complex was tested on the hormone-independent MDA-MB231 breast cancer cell line. Their studies showed the effect of concentration on the number of cancer dead cells. At low concentrations of 5 μM, there was a significant number of dead cancer cells compared to the high concentration dose of 200 μM. At 25 μM, the number of dead cancer cells increased drastically. At a high dose of 200 μM, it was observed that nearly all the cancerous cells were killed. Also, it is important to note that the diselenium (diSe) ligand was poorly active and these results were the combined effect of the Re–diSe complex on the cancer cells. Hence, the rhenium diselenoether complex could be considered as a potential drug for targeted anticancer treatment (Fig. 24).[68]

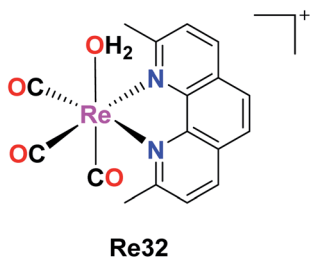

Re32

Fig. 23 Structure of the Re complex with the formula fac-[Re(CO)$_3$(2,9-dimethyl-1,10- phenanthroline)(OH$_2$)].

Rhenium metallocrown ether complex

The rhenium metallocrown ether with the formula [Re(CO)$_3$-Br(μ-pcatgd)] **Re34**, where pcatgd = 4-pyridine carboxylic acid tetra ethylene glycol diester was synthesized by Kumar *et al.* The cytotoxicity study of the synthesized **Re34** complex was not effective against peripheral blood mononuclear cells (PBMCs) and leukaemia. It was active against liver, lung and cervical cancer cells with IC$_{50}$ values of 9.2 μM, 18.2 μM and 63.7 μM, respectively. The **Re34** complex showed selective inhibition and potent anticancer activity against the MCF-7 (human breast cancer) cell line in a dose-dependent manner with the lowest IC$_{50}$ value of 11.9 μM compared to cisplatin. The ability of the **Re34** complex to target cancer cells may be due to its bio-conjugation to nano bodies and antibodies, which enabled it to deliver CO in larger amounts to cancer cells and tissues. Therefore, these researchers aim to study the structure–activity relationship of the **Re34** complex in the future (Fig. 25).[69]

Re(I) tricarbonyl triazine-based complexes

Ranasinghe *et al.* synthesized and reported four facial Re tricarbonyl complexes, [Re(CO)$_3$(H$_2$O)L1]$^+$ (**Re35a**), [Re(CO)$_3$L1Br] (**Re35b**), [Re(CO)$_3$(H$_2$O)L2]$^+$ (**Re35c**) and [Re(CO)$_3$L2Br] (**Re35d**), where L1 = 5,5′(3-(2-pyridyl)-1,2,4-triazine-5,6-diyl)-bis-2-furansulfonic acid disodium salt and L2 = (3-(2-pyridyl)-5,6-diphenyl-1,2,4-triazine-4′,4″-disulfonic acid sodium salt). The absorption spectra of these ligands showed isolated bands at 342–325 nm for L1 and L2 due to ligand-centered transitions. The emission spectra of the complexes displayed a weak fluorescent band in the visible region. For the cytotoxicity studies, **Re35(a–d)** was tested against rat peritoneal cells and no significant toxicity was observed for the **Re35a** and **Re35c** complexes, while **Re35d** showed the best results among the complexes. These complexes possessed enhanced luminescent properties (Fig. 26).[70]

Tosylhydrazone-based Re(I)(CO)$_3$ complexes

A novel series of organometallic tosylhydrazones with the general formula [{(η^5-C$_5$H$_4$)–C® = NNHSO$_2$C$_6$H$_4$CH$_3$}]Re(CO)$_3$, where R = H (**Re36a**) and CH$_3$ (**Re36b**), was synthesized by Concha *et al.* The cytotoxicity of the Re(I) complex was evaluated on the non-small lung cancer cell line (NSCLC). The IC$_{50}$ value of **Re36a** was found to be 37.5 μM, which had a cyrhetrenyl

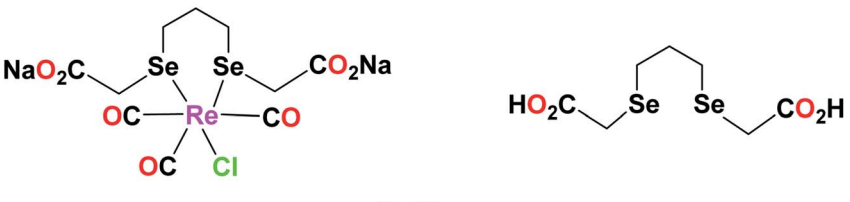

Re33

Fig. 24 Structure of the Re(I) diselenoether complex and its ligand.

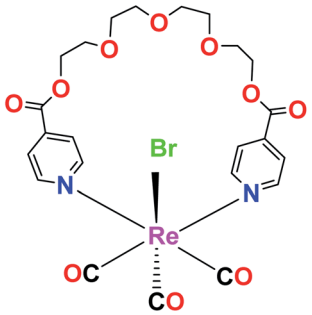

Re34

Fig. 25 Structure of Re complex with the formula [Re(CO)$_3$Br(μ-pcatgd)].

moiety. The antitumor activity of the complex increased for **Re36b** (IC_{50} = 24.3 μM). Their studies showed that the anti-proliferative activities were dependent on the electronic nature of the organic moiety and the substituent carbon of the hydrazone bridge. This phenomenon may be due to the inductive effect of the methyl group. The cytotoxicity of **Re36a** decreased (42.7 μM–134.0 μM) compared to the parent drug cisplatin (6.4 μM) on non-tumoral VERO cells. Also, the **Re36a** complex was observed to be more selective than the cisplatin drug (Fig. 27).[71]

Re(I) polypyridine complex for photodynamic therapy

The capability of Re(I) polypyridine complexes with the formula fac-[Re(et-isonic)(NN)(CO)$_3$]$^+$ (et-isonic = ethyl isonicotinate), NN = 1,10-phenanthroline (phen) **Re37a**, 4,7-dichloro-1,10-phenanthroline (Cl_2phen) **Re37c**, 4,7-dimethyl-1,10-phenanthroline (Me_2phen) **Re37b** or 4,7- diphenyl-1,10-phenanthroline (Ph_2phen) **Re37d**, to generate singlet oxygen in the presence of light and their localization in cells was studied by Ramos *et al.* Interestingly, the Re(I) complex was seen to function as an anticancer agent even in the absence of light. The human breast cancer cell line MCF-7 and melanoma cell lines SkMel-147 and SkMel-29 were considered for the study. The cytotoxicity of the Re(I) complexes was determined by the MTT assay. The IC_{50} values were in the order of 10^{-6} mol L^{-1} for the three studied human cell lines. The IC_{50} values for MCF-7, SkMeL-147 and SkMeL-29 were found to be 8.7, 6.1 and 4.6 μmol L^{-1}, respectively. These values were influenced by the N,N and axial ligand structure, which enhanced their active treatment, and also found to be better than cisplatin. The investigation of the cell death revealed that it occurred by apoptosis. The overexpression of the caspase-9 protein triggered the intrinsic pathway in apoptosis. The fac-[Re(et-isonic)(NN)(CO)$_3$]$^+$ complex displayed higher lipophilicity and higher cytotoxicity than the uncharged fac-[ReCl(Ph_2-phen)(CO)$_3$] complex. The synthesized Re(I) complexes also exhibited emission properties. It was observed that the emission properties originated from the ^{3}MLCT (metal to ligand charge transfer), which was sensitive to the N,N ligand (Fig. 28).[72]

PTA-based Re(I) tricarbonyl complexes

Marker *et al.* synthesized and reported fifteen water-soluble **Re38(PTA1–5)**, **Re38(THP1–5)**, **Re38(DAPTA1–5)** Re(1)tricarbonyl complexes with the general formula [Re(CO)$_3$(-NN)(PR_3)]$^+$, where N,N is a diimine ligand and PR_3 is 1,3,5-triaza-7-phosphaadamantane (PTA), tris(hydroxymethyl)

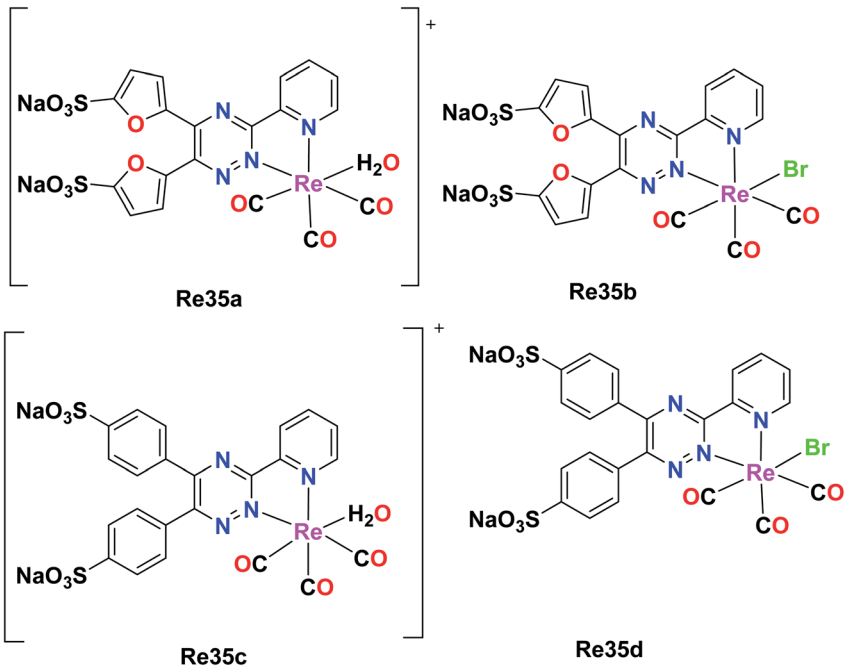

Re35a Re35b Re35c Re35d

Fig. 26 Structures of Re tricarbonyl complexes with the general formula [Re(CO)$_3$(H_2O)(L)] and[Re(CO)$_3$(L)Br].

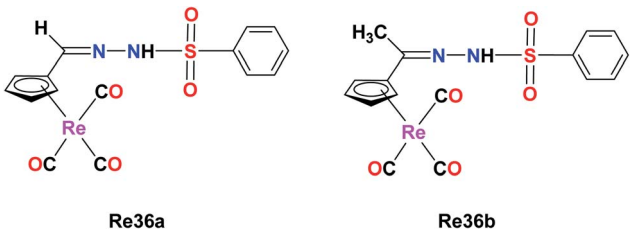

Fig. 27 Structure of Re complex with the formula [{(η^5-C_5H_4)–C® = $NNHSO_2C_6H_4CH_3$}]$Re(CO)_3$.

phosphine (THP) or 1,4-diacetyl-1,3,7-triaza-5-phosphabicylco [3.3.1]nonane (DAPTA). The THP and DAPTA ligands exhibited triplet-based luminesce. For the biological studies, these complexes were evaluated against A2780 and A2780CP70. The studies revealed that these complexes could induce cytotoxicity through covalent interactions with biomolecules. Complex **Re38(DAPTA1)** was the most potent compound among the synthesized compounds, having $IC_{50} = 6$ μM. The production of O_2 was also observed (Fig. 29).[73]

Tricarbonyl rhenium isonitrile polypyridyl complexes

Vaughn *et al.* synthesized 11 rhenium tricarbonyl complexes with the general formula fac-$[Re(CO)_3(NN)(ICN)]^+$, where N,N = chelating diimine and ICN = isonitrile ligand explored their anticancer activities. The cytotoxicity of the 11 tricarbonyl rhenium isonitrile polypyridyl (TRIP) complexes was tested on HeLa cells by the MTT assay. The cytotoxicity values of these 11 complexes were in the range of 1.2 μM to 53 μM. The **Re39f** complex $[Re(CO)_3$(4,4′-bis(trifluoromethyl-2,2′-bipyridine))(*p*-tolyl ICN)], where ICN is an isonitrile moiety, was observed to be very inactive on HeLa cells with an IC_{50} value of 53 μM. This was due to the presence of the weakly electron-donating 4,4-bis(trifluoromethyl-2,2-bipyridine) ligand. The **Re39e** complex $[Re(CO)_3$(4,4-dimethoxy-2,2-bipyridine)(*p*-tolyl ICN)] showed an IC_{50} value of 8.4 μM due to the presence of more electron-rich 4,4-dimethoxy-2,2-bipyridine ligand. Based on these observations, it was concluded that the cytotoxicity of the complexes varied depending on the electron density of the compounds. However, the **Re39g** complex $[Re(CO)_3$(4,4-di-*tert*-butyl-2,2-bipyridine)(*p*-tolyl ICN)] showed higher activity than the **Re(5)** complex due to the presence of the lipophilic and bulky (4,4-di-*tert*-butyl-2,2-bipyridine) ligand. Thus, it was observed that the steric factor and lipophilicity also influenced the cytotoxicity of the complexes together with electronic factors. The maximum cytotoxic activity among the complexes was shown by the **Re(1)** complex $[Re(CO)_3$(2,9-dimethyl-1,10phenanthroline)(*p*-tolyl ICN)$]^+$ with an IC_{50} value of 1.4 μM in HeLa cells. However, the *in vivo* anticancer activity in mice showed that **Re39a** was unable to eradicate the tumor mass. Therefore, it was apparent that the more electron-rich compounds were more cytotoxic. The isonitrile ligands did not influence the cytotoxicity of the complexes to a significant extent. It was observed that the complexes possessing a greater C–N stretching showed lower cytotoxic activity. The TRIP complexes triggered the cell death of cancer cells by creating ER (endoplasmic reticulum) stress (Fig. 30).[74]

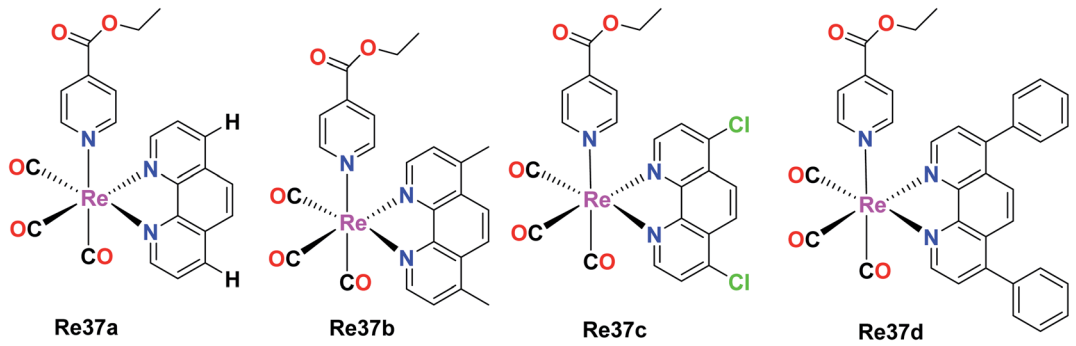

Fig. 28 Structure of rhenium complexes with the formula fac-[Re(et-isonic) (NN)$(CO)_3]^+$.

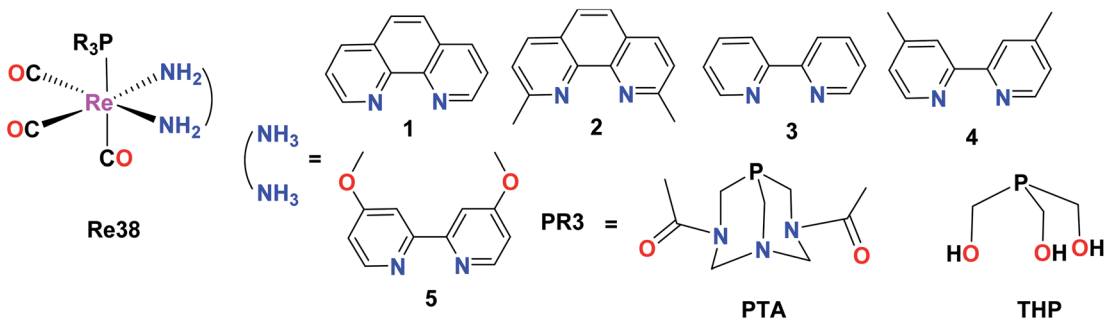

Fig. 29 Structure of Re complex with the general formula $[Re(CO)_3(NN)(PR_3)]^+$.

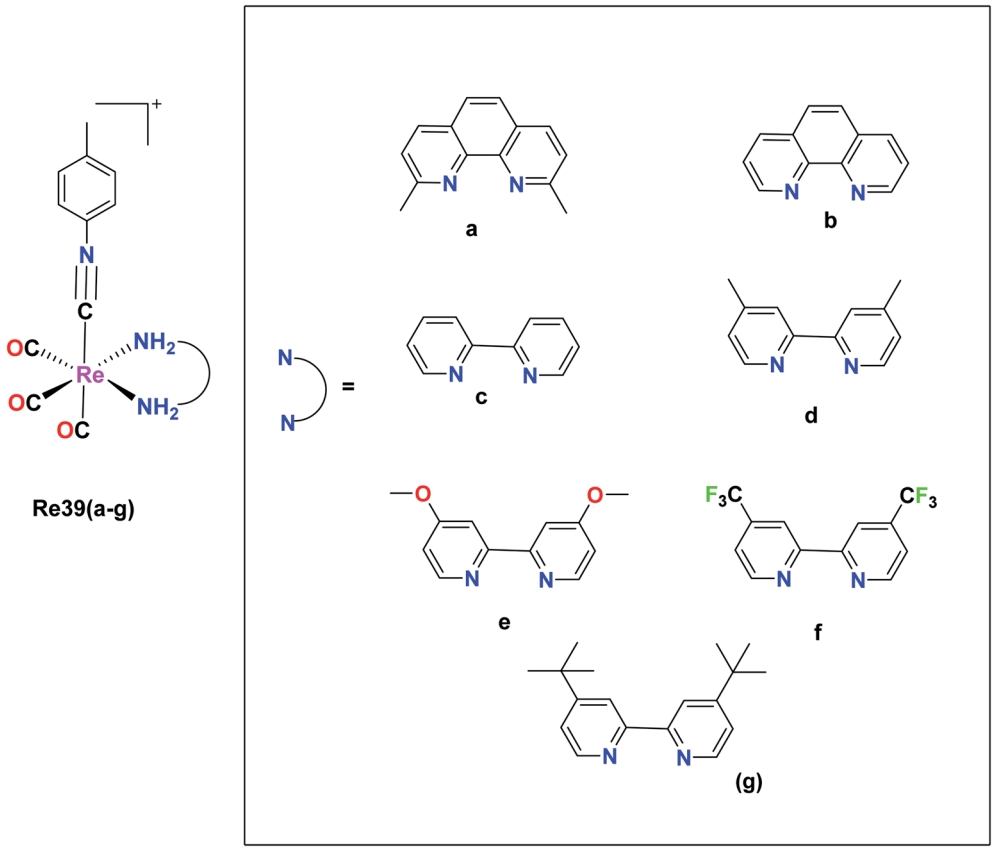

Fig. 30 Structure of Re tricarbonyl complex with the formula fac-$[Re(CO)_3(NN)(ICN)]^+$.

A new Re(I) tricarbonyl complex having a chelating polypyridine ligand and an isonitrile ligand was reported by King *et al.* The **Re40** complex with the formula $[Re(CO)_3(dmphen)(p\text{-tol-ICN})]^+$, where dmphen is 2,9-dimethyl-1,10-phenanthroline and *p*-tol-ICN is *para*-tolylisonitrile, was tested for cytotoxicity against various cancer cell lines including ovarian cancer (A2780), cisplatin-resistant ovarian cancer (A2780CP70), A549 embryonic kidney fibroblasts (HEK293), cervical, and lung cancer, exhibiting good results with IC_{50} values of 1.7 μM, 1.9 μM, 1.4 μM, 1.4 μM and 1.9 μM, respectively. **Re(1)** exhibited good results in melanoma and breast cancer cell lines compared to lung and renal cancer cell lines, where it was the least effective. The **Re40** complex triggered the accumulation of misfolded proteins, which caused endoplasmic reticulum (ER) stress, unfolded protein response and caspase-induced apoptotic cell death. The current efforts of these researchers are being directed towards the synthesis of different complexes to develop a structure–activity relationship and performing proteomics studies to identify the molecular mechanism of action of **Re40** (Fig. 31).[75]

Santoro *et al.* synthesised tris-carbonyl diimine fluorescent rhenium complexes (Fig. 32a) with the general formula fac-$[Re(CO)_3(Me_2\text{-phen})]^+$, where Me_2-phen = 4,7dimethyl-1,10 phenanthroline. The synthesized **Re41a** and **Re41b** complexes were adducts of vitamin B12. The cytotoxicity of the synthesized rhenium complexes was evaluated on PC-3 (prostate cancer cell line). The cytotoxicity of **Re41a** and **Re41b** and the pristine complex $[Re(CO)_3(Me_2\text{-phen})MeOH][NO_3]^-$ **Re41c** was in the lower micro molar range. Among the complexes, **Re41a** was found to be most active. The least active **Re41b** had an average

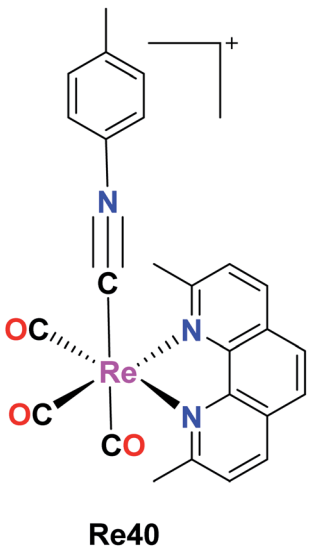

Fig. 31 Structure of $[Re(CO)_3(dmphen)(p\text{-tol-ICN})]^+$.

IC_{50} value of 15 μM. The cytotoxicity evaluation of the **Re41(a–c)** complexes was extended to 3T3 fibroblasts. The complexes showed a similar trend of cytotoxicity towards 3T3 fibroblasts as that to PC-3 cells. **Re41b** showed no cytotoxicity against fibroblasts. The IC_{50} value for **Re41b** and **Re41b** was in the range of 50 μM. The cellular localization studies showed that **Re41b** was more concentrated in the proximity of the nucleus, and also present in the cytoplasmic region. **Re41a** was not stable in the cell media. The emission spectra of the rhenium complexes were attributed to the ligand centered (^{1}LC) transition and metal to ligand charge transfer (^{1}MLCT). However, the complexes were not suitable for fluorescence imaging given that the absorption of vitamin B12 overlaps with the emission of **Re41a**, resulting in a very low quantum yield.[76]

β-Carboline Re(I) complexes

Maisuls *et al.* reported β-carboline Re(I) complexes fac-$[Re(CO)_3(dppz)(nHO)]O_3SCF_3$ and fac-$[Re(CO)_3(nHO)_3Cl]$ where dppz = dipyrido[3,2-*a*:2,3-*c*]phenazine and nHO = 9*H*-pyrido[3,4-*b*]indole (norharmane). fac-$[Re(CO)_3(dppz)(nHO)]^+$ (**Re42a**), fac-$[Re(CO)_3(nHO)2Cl]$ (**Re42b**), fac-$[Re(CO)_3(bpy)(nHO)]^+$ (**Re42c**) and fac-$[Re(CO)_3(phen)(nHO)]^+$ (**Re42d**). The **Re84(a–d)** complexes were tested against A549 cells for *in vitro* cytotoxicity studies and the results showed a gradual increase in cytotoxicity in the order of **Re42a** (IC_{50} = 10 μM) < **Re42d** (IC_{50} = 65 μM) < **Re42c** (IC_{50} = 85 μM) < **Re42** (IC_{50} = 88 μM). The intrinsic cytotoxicity of the complexes depends upon the chemical nature of the accompanying ligand complexes rather than the net charge of the molecules. Their studies showed that the $Re(CO)_3$

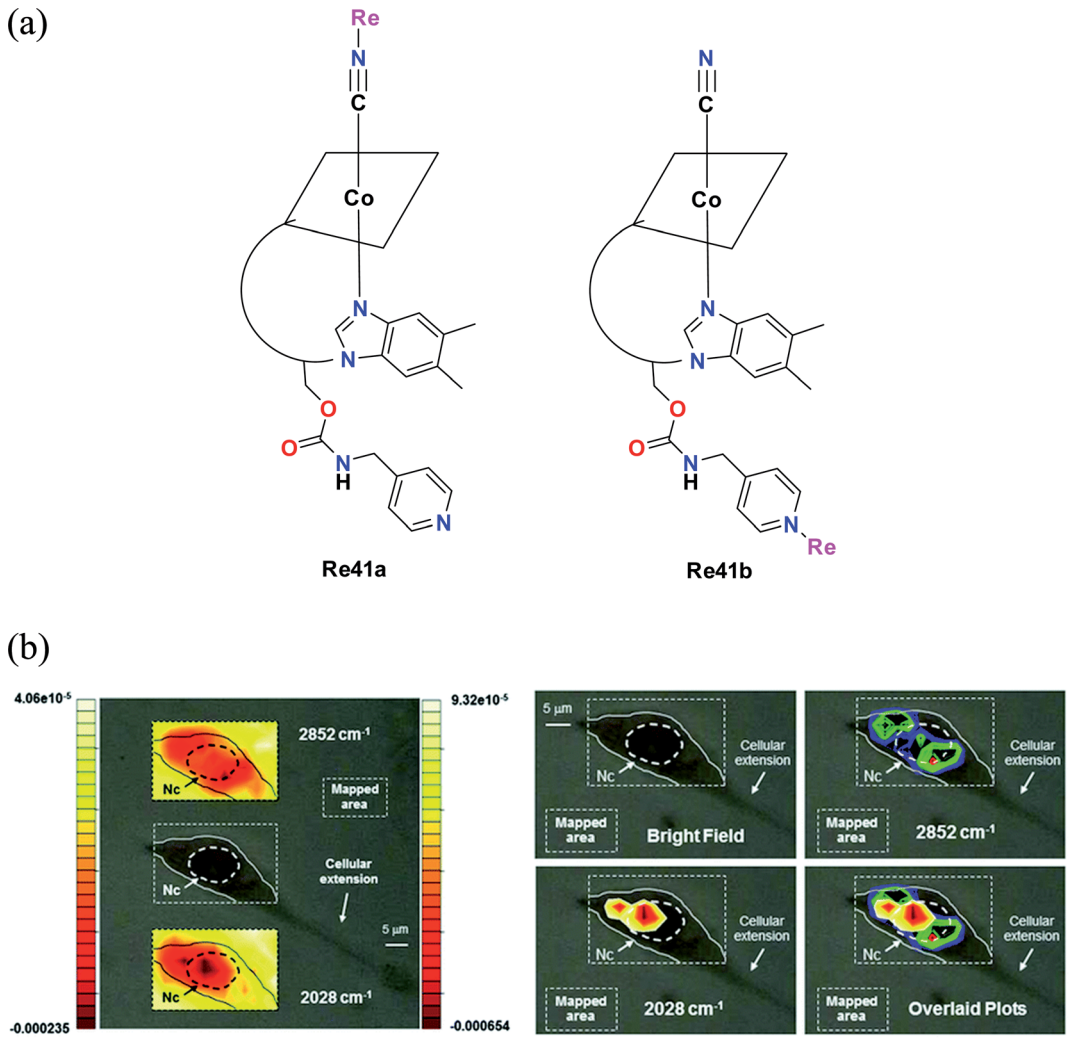

Fig. 32 (a) Structure of Re complexes with the formula $[Re(CO)_3(Me_2\text{-phen})]^+$. (b) Optical images of a 3T3 fibroblast incubated with **41b** (300 μM concentration). Left: top and bottom insets show the contour images reconstructed from mapping the intensities of the 2nd derivative of the lipid absorption at 2852 cm^{-1} and the A1 carbonyl stretching vibration at 2028 cm^{-1}, respectively. The scales represent relative units of the 2nd derivative of the absorbance with the left scale referring to the top inset. Nc = cell nuclear area identified as previously described. Right: same cell with maximum of reconstructed integrated contour intensities (same scale as the left with minimum set to -9.5×10^{-5} and −0.00024 units for the 2852 cm^{-1} and the 2028 cm^{-1} vibrations, respectively) of the 2nd derivative of the same lipid absorption and the A1 stretching frequency finally superimposed in the bottom right panel to highlight the different chemical distributions of the molecular species. Pixel maps of the same images may be found in the ESI. [Adapted from ref. 76 from The Royal Society of Chemistry.]

core of the nHO ligands increased the cytotoxicity of the βC moiety of the A549 cells. **Re42a** showed the best result, which was due to intrinsic intercalative property of the dppz ligand with DNA. **Re42c** and **Re42d** showed moderate cytotoxicity on A549 cells. These complexes had high hydrophobicity and may be localized in hydrophobic intracellular compartments such as mitochondria, lysosomes, and Golgi body. Given that they were highly hydrophobic, they were suitable for micelle-based drug delivery. These complexes displayed an intense band in the range of 2100–1800 cm^{-1}. **Re42(a–d)** showed no evidence of cell death (Fig. 33).[77]

Rhenium(I) tricarbonyl bimetallic complexes

Two pairs of complexes, mononuclear (**Re43a** and **Re43b**) and dinuclear (**Re43c** and **Re43d**) phosphorescent organometallic **Re43(a–d)** tricarbonyl complexes were synthesized and designed as efficient anticancer agents by Ye *et al.* The synthesized homonuclear complexes **Re43a–Re43b** with the general formula $[Re(N–N)(CO)_3(L)]PF_6$, where N–N = 1,10 phenanthroline and L = 1,2-bis(4-pyridyl)-ethane and dinuclear complexes **Re43c–Re43d** with the general formula$[(N–N)(CO)_3Re(L)Re(CO)_3(N–N)](PF_6)_2$, where **Re43c**: N^N = phen; **Re43d**: N^N = DIP were investigated for their cytotoxic activity against LO2 (human normal liver cell line), HePG2 (human hepatocellular liver carcinoma), A549R (cisplatin resistant), A549 (human lung adenocarcinoma epithelial cell line) and HeLa (human cervical cancer cell line). Reportedly, the **Re43c** complex showed greater activity than cisplatin for all the tested cancer cell lines. Among the four complexes, **Re43b** and **Re43d** displayed greater anticancer activity than **Re43a** and **Re43c** and the platinum drug cisplatin. The A549R cancer cell line is resistant towards cisplatin. However, the **Re43d** complex showed remarkable anticancer potency, nearly 38 times higher potency to kill the cisplatin-resistant A549R cells. The **Re43b**, **Re43d** and **Re43c** complexes exhibited 5 times lower cytotoxicity against LO2 cells than HePG2 cells. The lipophilicity of the complexes influenced their cellular localization. The complexes with higher lipophilicity, namely **Re43b** and **Re43d**, were seen to localize in the mitochondria, whereas **Re43c** was localized in the lysosomes due to its lower lipophilicity. The scope of cellular uptake for **Re43c** and **Re43d** was extremely higher than that of **Re43a** and **Re43b**. The cell death studies showed that the lysosome-localized **Re43a** complex induced the caspase-independent apoptosis pathway, whereas the mitochondria-localized **Re43d** complex induced the caspase-independent paraptosis. Therefore, the subcellular localization of the complexes was fully dependent on the structure of the complexes (Fig. 34).[31]

Wang *et al.* reported two binuclear Re(I) complex with the formula $[Re_2(CO)_6(dip)_2L](PF_6)_2$ (dip = 4,7-diphenyl-1,10-phenanthroline; L = 4,4-azopyridine (**Re44a**) or 4,4-dithiodipyridine (**Re44b**)). These complexes possessed intense absorption bands at around 260–300 nm due to the inter ligand π–π* transitions. **Re44a** and **Re44b** were tested against several cell lines including A549, A549R, HeLa, HepG2, U2SO (human osteosarcoma), PC3 and LO2 (human normal liver) and acquired high anticancer activities. The cytotoxicity of **Re44b** for all the cells lines was between IC_{50} = 0.8 μM–2.1 μM. **Re44a** was the least toxic in HePG2 and PC3 (IC_{50} > 25 μM). These complexes exhibited better cytotoxicity results compared to cisplatin and could kill A549 cells, indicating their efficiency to overcome CDDP-induced resistance. They were mainly accumulated in the mitochondria (they can target and depolarize mitochondria), causing oxidative stress and mitochondrial dysfunctional, slowing down the bioenergetic rate. The GSH metabolism and redox homeostasis were disturbed by the impacted redox-related enzymes. **Re44a** and **Re44b** also induced necroptosis and caspase-dependent apoptosis and the inhibition of tumor growth. They also affected anticancer stress by irreversible oxidative stress and cellular redox imbalance (Fig. 35).[78]

Pan *et al.* reported Re(I) tricarbonyl complexes [**Re45(a–b)**] (Fig. 36a) with β-carboline derivatives. For the cytotoxicity study, these complexes were tested against cell lines including A549, A549R, HeLa, MCF-7 and HLF (human lung fibroblasts) and their cytotoxicity values were seen to range between 2.2 μM and 15 μM. **Re45a** and **Re45b** showed higher anticancer activity than that of cisplatin. **Re45b** (IC_{50} = 4 μM) was 2 times more active compared to cisplatin in A549 cells and 3.4 times more than **Re45a**, which was probably due to the greater cellular uptake efficiency of **Re45b**. The **Re45b** complex showed higher antiproliferative activities against cisplatin-resistant A549R cells and also increased the production of intracellular ROS (H_2O_2

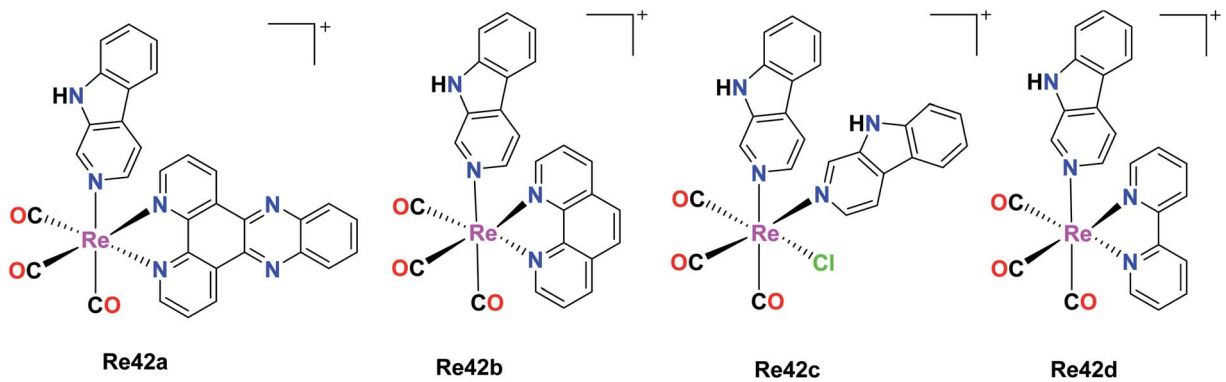

Fig. 33 Structure of Re tricarbonyl complexes with the general formula fac-$[Re(CO)_3(L)(nHO)]^+$.

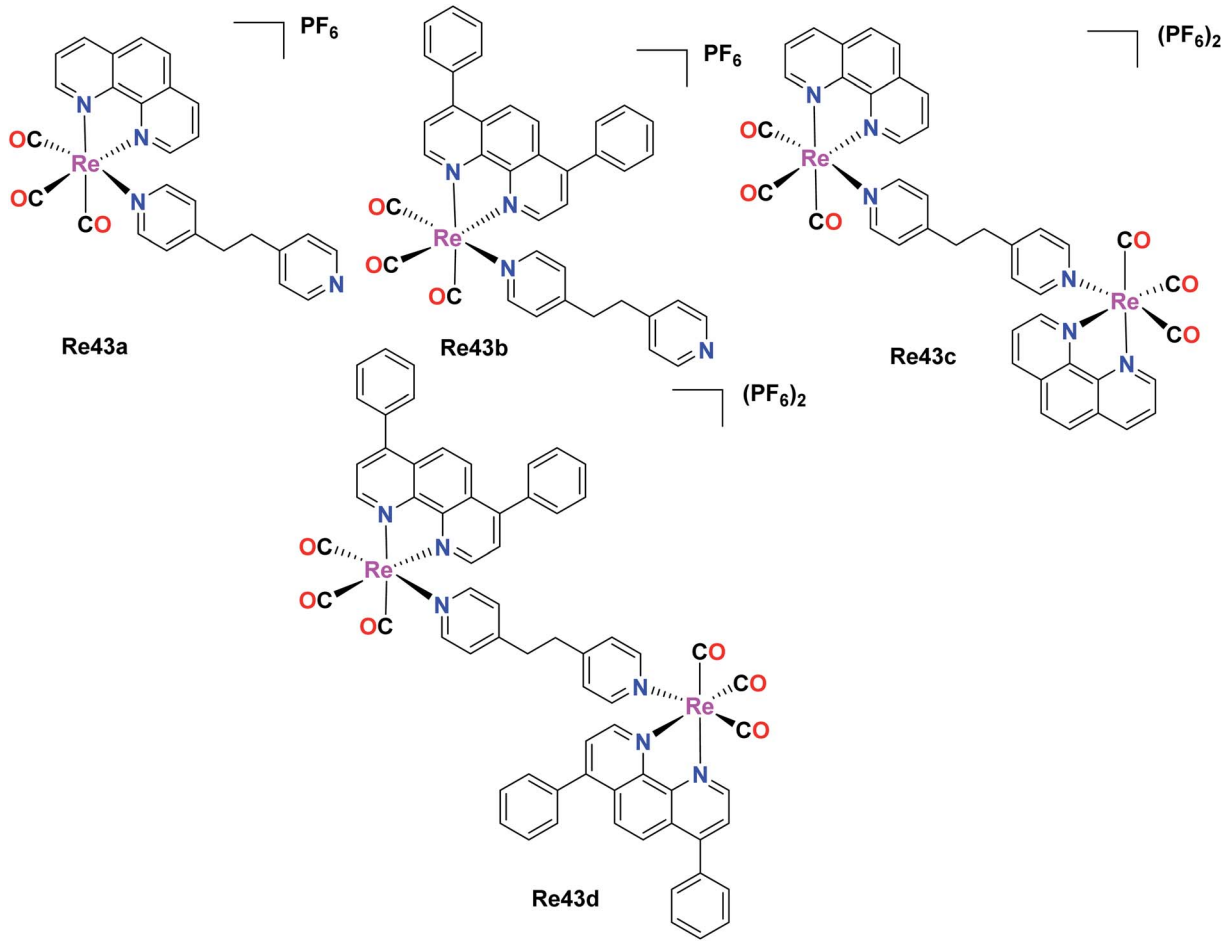

Fig. 34 Structure of Re mononuclear complexes with the general formula $[Re(N-N)(CO)_3(L)]PF_6$ and dinuclear complexes with the general formula $[(N-N)(CO)_3Re(L)Re(CO)_3(N-N)](PF_6)_2$.

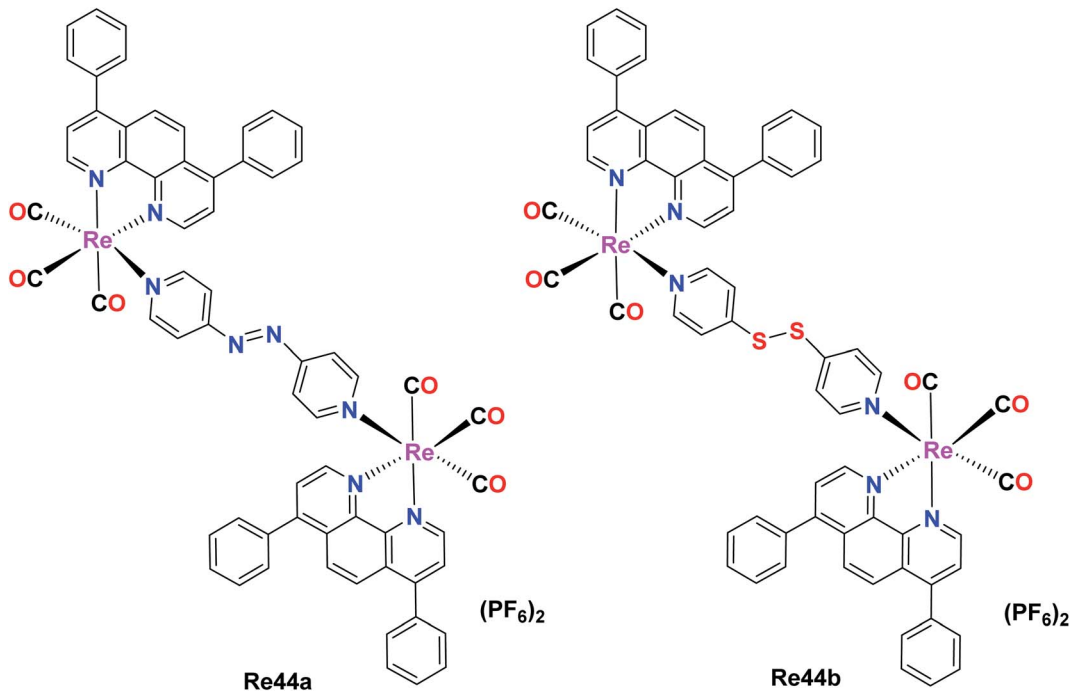

Fig. 35 Structure of Re complexes with the formula $[Re_2(CO)_6(dip)_2L](PF_6)_2$.

and super oxide ion radicals are key ROS), leading to the destruction of the lysosomal membrane. The colocalization experiment also demonstrated that the cellular fluorescence of the complexes was nicely overlapped with LysoTracker Green, whereas insignificant overlap was found in the case of Mito-Tracker Green (Fig. 36b). **Re45b** induced morphological changes, and thereby cell death. **Re45a** and **Re45b** displayed significant phototoxicity under light (425 nm) irradiation in A549 cells.[79]

Giffard *et al.* synthesized and reported mono and multi-nuclear [2 + 1] Re tricarbonyl complexes **Re46(a–c)**, which were tested against A31, A431, colon carcinoma (DLD-1), A2780, and fibroblast cells (BJ) by the MTT assay for *in vitro* cytotoxicity studies. All the complexes showed good results with the A2780, A431, and DLD-1 tumor cell lines. **Re46c** showed the best inhibitory results against the tested cell lines, whereas **Re46a** did not show selectivity. However, **Re46b** and **Re46c** showed selectivity with a good therapeutic window. **Re46c** was particularly selective against the A2780 cell line. The cytotoxicity was found to follow the order of **Re46c** > **Re46b** > **Re46a**. It was evident that **Re46a** had one metal centre, **Re46b** had three metal centres, and **Re46c** had four metal centres. The IC_{50} values of the complexes against A431 were **Re46c** (14 μM), **Re46b** (46 μM), and **Re46a** (57 μM). These complexes could induce programmed cell death in tumour cells. **Re46c** was more recognized in the bax-α modulator in all the cell lines (Fig. 37).[80]

Amide-functionalised Re(I) dinuclear metallacycles

R. Govindarajan *et al.* synthesized the **Re47(a–d)** complexes with the formula $[Re(CO)_3(\mu\text{-N–L–N})Br]2$, where N–L–N is a ditopic amide-functionalised ligand. These complexes showed selective anticancer activities towards cancer cell lines. The effect of these Re(I) complexes was tested on the leukaemia (K562), liver (HepG2), colon (HCT-15), cervical (HeLa) and lung (A549) cancer cell lines. The ditopic amide ligands (**L1–L4**) incorporated in the **Re47(a–d)** complexes were hydrophobic moieties in the metallacyclic framework, which played an important role in the

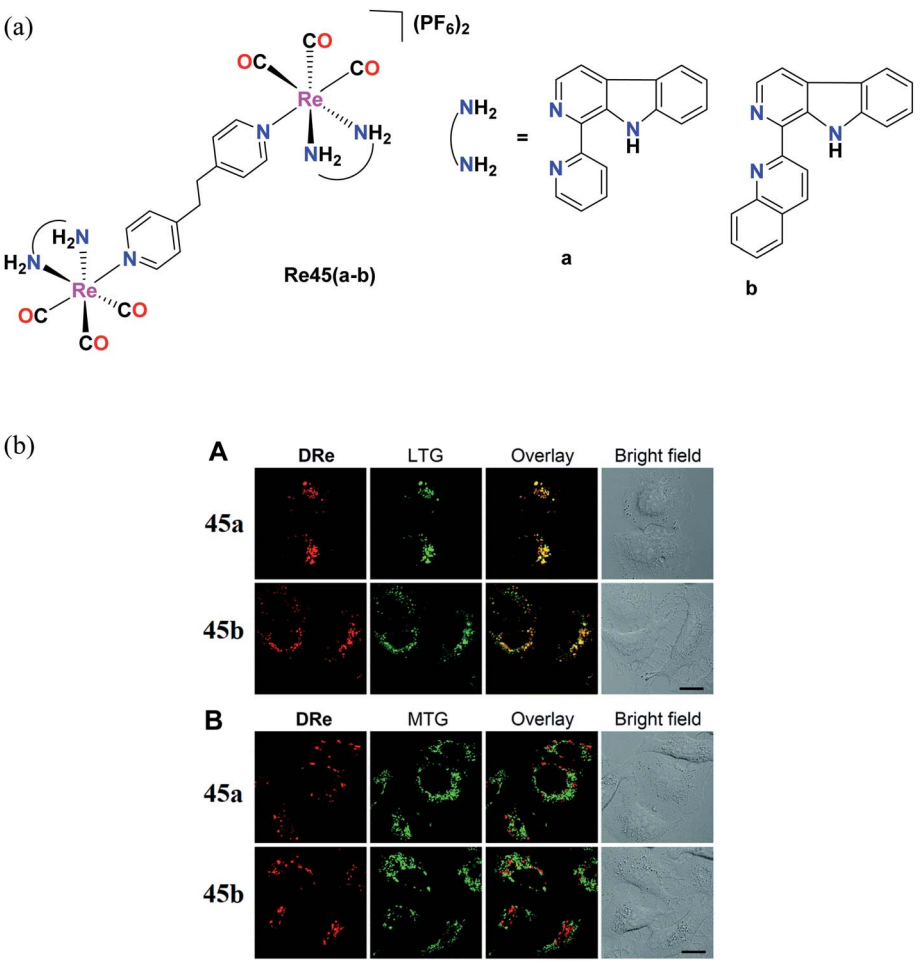

Fig. 36 (a) Structure of Re complexes with the general formula $[(L)(CO)_3Re(BPE)Re(CO)_3(L)](PF_6)$. (b) (A) Confocal images of A549 cells co-labeled with **45a** (20 μM, 1 h), **45b** (5 μM, 1 h) and LysoTracker Green DND-26 (LTG; 150 nM, 0.5 h). (B) CLSM images of A549 cells co-labeled with **45a** (20 μM, 1 h), **45b** (5 μM, 1 h) and MitoTracker Green FM (MTG; 150 nM, 0.5 h). $\lambda_{ex} = 488$ nm (LTG and MTG) and 405 nm (**45a** and **45b**); $\lambda_{em} =$ 550–600 nm (**45a**), 600–650 nm (**45b**), and 490–530 nm (LTG and MTG). All images share the same scale bar: 20 μm. [Adapted from ref. 79 with permission from The Royal Society of Chemistry.]

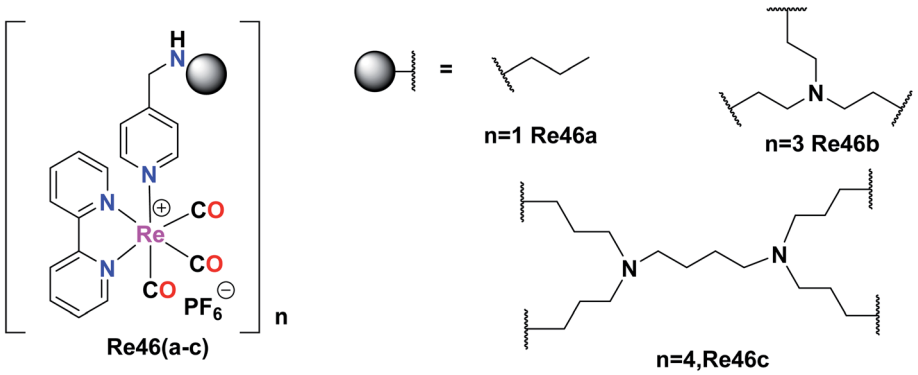

Fig. 37 Structure or Re(I) multinuclear tricarbonyl complexes with the general formula $[Re(bpy)(CO)_3]$.

anticancer activity of the complexes. The complexes with greater hydrophobic groups and flexibility exhibited good anticancer activity. The **Re47c** and **Re47d** complexes showed comparable cytotoxicity to the cisplatin drug. The cytotoxicity of **Re47c** was 22.8 μM, 29.4 μM and 26.4 μM towards cervical, liver and leukaemia cancer cell lines, respectively. The **Re47d** complex was active towards all the cell lines and showed IC_{50} values of 24.7 μM, 21.2 μM, 22.1 μM, 27.3 μM and 24.1 μM. The **Re47a** and **Re47b** complexes also showed broad anticancer activities with IC_{50} values of less than 50 μM. The Re(I) complexes showed inhibitory potency following the order of **Re47a** < **Re47b** < **Re47c** < **Re47d**. **Re47a** and **Re47b** displayed broad spectrum anticancer activities. The anti-proliferative activity of these synthesized compounds was measured with the help of the MTT assay. The complexes induced programmed cell death in cancer cells. The mechanism of the anticancer activity of the **Re47c** and **Re47d** complexes is yet to be studied and expected to form the future basis for further research (Fig. 38).[81]

Dinuclearmetallocyclophanes

Kumar and group synthesised dinuclearmetallocyclophanes of the type $[Re(CO)_3Br(\mu\text{-}L)]_2$ (L = ligand), L1 = 1,2 phenylene diisonicotinate(Pdi) **Re48a** and L2 = bis(4-(4-pyridylcarboxyl) phenyl)dimethymethane (bpcpd) **Re48b** and investigated their cytotoxic activity on various cancer cell lines namely HeLa (cervical cancer), HepG2 (liver cancer), leukemia (K562) and many other cancer cell lines. Among these cell lines, the Re(1) complex showed effective cytotoxicity against the HepG2 liver cancer cell line, while the cytotoxicity of the **Re48b** complex was effective against the HeLa cell line. The IC_{50} value was recorded to be 14.2 μM and 12.4 μM for **Re48a** and **Re48b** against the tested cell lines, respectively. These values were better than that of cisplatin, indicating the potential anticancer activity of the synthesised complex. The anticancer activity of these complexes against the liver and cervical cancer cell lines was thought to be

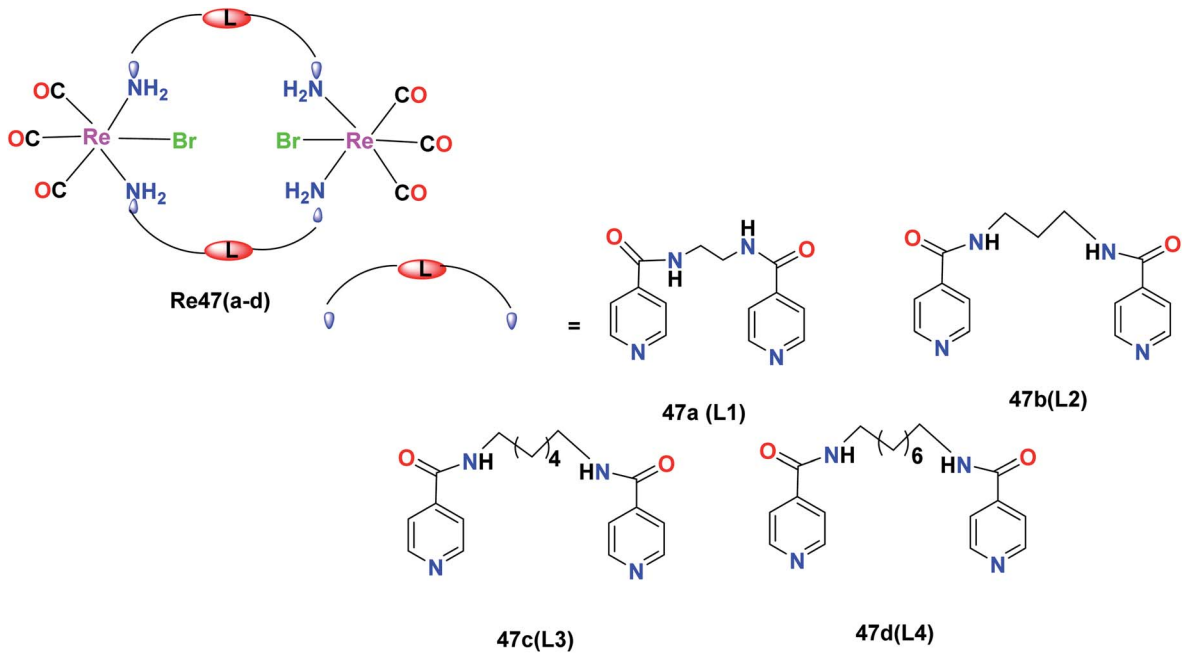

Fig. 38 Structure of Re complexes with the formula $[Re(CO)_3(\mu\text{-}N\text{-}L\text{-}N)Br]_2$.

due to the induction of apoptosis but this is yet to be ascertained by researchers (Fig. 39).[82]

Luminescent Re(I)-based heterobimetallic complexes

The anticancer studies of luminescent Re(I) complexes were investigated by Luengo *et al.* on the A549 (lung cancer) cells and HeLa (cervix cancer) cells. Their work aimed to synthesize novel heterotrimetallic complexes possessing potential to expose the precise time of complex-biological target interaction. Thus, neutral and cationic variants of the heterotrimetallic Re(I)/Au(I) complexes were synthesized together with their monometallic Re(I) precursors. The photophysical studies revealed a similar absorption pattern for all seven synthesized complexes. The measured absorptions were due to the ligand centered transitions (^{1}LC) and metal to ligand charge transfer transitions (^{3}MLCT) at lower energies. The emission measurements showed similar results with a broad band between 565 nm and 680 nm. The emission band was also due to ^{3}MLCT transitions from dπ (Re) → π* (LNN). The LNN ligand was the key ligand that connected the Re metal and the gold metal. A noteworthy observation in the photophysical studies was that the **Re49a** and **Re49f** monometallic Re(I) precursors exhibited maxima at lower

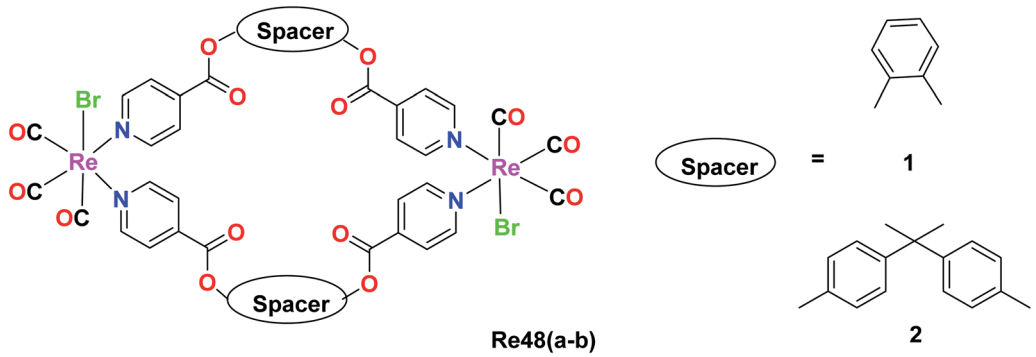

Fig. 39 Structure of Re tricarbonyl complex with the formula $[Re(CO)_3Br(\mu\text{-}L)]_2$.

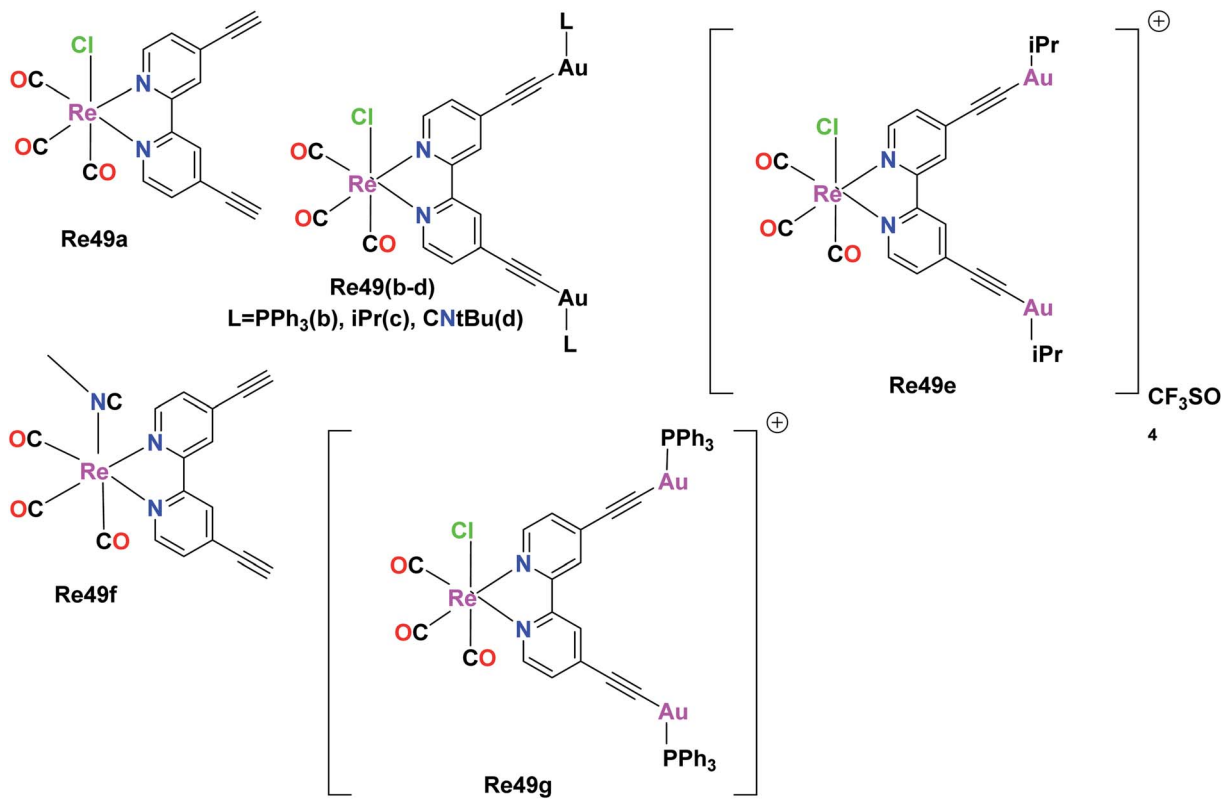

Fig. 40 Structures of Re complexes with the formula fac-$[Re(CO)_3(biPy(CC)_2\text{-}(AuL)_2)X]^n$.

energies than the cationic (**Re49e–Re49g**) and neutral (**Re49b–Re49d**) heterotrimetallic analogues. This is because the gold fragment renders extra electron density to the diimine. The anti-proliferative studies of the **Re49(a–f)** complexes were determined by the MTT assay in the A549 and HeLa cell lines. The anti-proliferative activity of the heterometallic complexes was more selective towards HeLa cells than the monometallic complexes. Also, the cytotoxicity of the neutral species was less than that of the cationic species. The neutral heterotrimetallic complexes **Re49b** and **Re49d** showed selective cytotoxicity towards HeLa cells, with the cytotoxicity values of 6.46 μM and 10.79 μM, respectively. The cytotoxicity value of the **Re49c** complex was greater than 25 μM, which was an exception. The selectivity and higher toxicity towards the HeLa cell line over the A549 cell line could be possibly due to the interaction of the solid compound with the outer cellular membrane. Complex **1** showed anti-proliferative activity towards both A549 and HeLa cells. The **Re49f** complex showed similar anti-proliferative activity to complex **1** with an excellent cytotoxicity value of <8 μM. This superior IC_{50} value of the cationic Re(I) complex **Re49f** can be attributed to its higher solubility. The heterotrimetallic cationic complexes **Re49e** and **Re49g** did not show selective inhibition towards the proliferative activity of HeLa cells in contrast to their neutral analogues **Re49b** and **Re49d**. The cytotoxicity behavior of the Re(I) complexes followed the order of $-PPh_3$ > –CNtBU > –IPr. The greatest cytotoxicity was shown by the phosphine derivative. This is because the gold ancillary ligands modulate the cellular uptake given that they have different lipophilic and hydrophilic characters, which are important for the transport of the cytotoxic agent. The cellular uptake of the cationic complex **Re49g** was twice that of its neutral analogue **Re49b**. This reveals that the cationic nature of the complex is essential for its internalization. Consequently, future heterometallic complexes can achieve specific targeting and solubility *via* the introduction of small amino, peptide and water-soluble groups (Fig. 40).[83]

3. Conclusion

This review presented the importance of anticancer properties of different rhenium-based organometallics and rhenium tricarbonyl complexes in the field of anticancer research. Besides being a promising candidate for anticancer drugs, rhenium complexes also exhibit striking luminescent and phosphorescent properties, and thus these complexes can be employed for imaging and tracking the morphological changes induced in the targeted organelles of cancer cells inside the body. Special attention has been given to bis(quinolinoyl) Re(I) tricarbonyl complexes given that they do not need any external fluorophore for tracing them inside cancer cells by confocal imaging.[84] These complexes exhibit very low toxicity on normal cells, and therefore have been identified as cytoselective agents. The literature values of cytotoxicity for most rhenium complexes show that they are better than the platinum-based cisplatin drug. Moreover, the lipophilicity of these complexes has a major influence on their cytotoxicity, where their cytotoxicity may increase with an increase in the lipophilicity of their ligands. Also, the concentration of the complex affects its cytotoxicity. It has been shown that all cancer cells can be killed at an optimum concentration range of these complexes. Hence, tuning these two factors can establish rhenium complexes as highly effective anticancer drugs in the future. Some rhenium complexes are also active on cell lines that are cisplatin resistant. Briefly, it can be concluded that rigorous research on the development of rhenium complexes for theranostic applications will provide a breakthrough in the field of cancer therapy.

Conflicts of interest

There are no conflicts to declare.

Abbreviations

LO_2	Human normal liver cell line
HeLa	Cervical cancer cell line
A549	Human lung carcinoma
A549R	Cisplatin-resistant human lung carcinoma
HSA	Human serum albumin
PC3	Human prostate carcinoma
MCF-7	Human breast cancer
A2780	Human ovarian carcinoma
^{3}MLCT	Triplet metal to ligand charge transfer
HCT	Colon tumor cancer
MLCT	Metal to ligand charge transfer
MTT	3-(4,5-Dimethylithiazol-2-yl)-2,5-diphenyltetrazolium bromide
NADH	Nicotinamide adenine dinucleotide
BSA	Bovine serum albumin
ROS	Reactive oxygen species
MMP	Mitochondria membrane potential
Hep G2	Human liver cancer cell line
BEL 7402	Human hepatoma cell line
HCT-116	Colon cancer cell line
ATP	Adenosine triphosphate
DNA	Deoxyribonucleic acid
ER	Endoplasmic reticulum
LC	Ligand centre
B16	Melanoma cells
PDT	Photodynamic therapy
HLF	Primary human lung fibroblasts
MDB-MA-231	Human breast cancer cell line
SGC-7901	Human gastric cancer cell line
A2780	Ovarian cancer cell line
A2780CP70	Ovarian cancer cell line
MRC5	Lung cancer cell line
NSCI-H460	Non small lung cancer
MIA Pa Ca 2	Pancreatic carcinoma cells
HUVECs	Human umbilical vein endothelial cells
U2S0	Human osteosarcoma
HEK-293	Human embryonic cells
DLD-1	Colon carcinoma
HDAC7	Human recombinant cells

HT-29	Colorectal adenocarcinoma
SkMeL-147	Melanoma cell line
SkMeL-29	Melanoma cell line
LOVO	Colon adenocarcinoma
PBMC	Peripheral blood mononuclear cells
MDA-MB-231	Breast cancer cell line
K562	Leukemia
HCT-15	Colon cell line
HTB-12	Brain cancer cells
D54	Human glioblastoma cell line
VERO	Kidney epithelial cells
LDH	Lactate dehydrogenase

Acknowledgements

The authors gratefully acknowledge VIT for providing'VIT SEED GRANT', Vellore for the support through Seed Grant for Research. We acknowledge DST-SERB CRG (CRG/2021/002267) grant for funding. We acknowledge DST, New Delhi, India for DST-FIST project.

References

1 B. S. Murray and P. J. Dyson, Recent progress in the development of organometallics for the treatment of cancer, *Curr. Opin. Chem. Biol.*, 2020, **56**, 28–34.
2 S. Mcguire, World Cancer Report 2014, Geneva, Switzerland, World Health Organization, International Agency for Research on Cancer, WHO Press, 2015, *Adv. Nutr.*, 2015, **7**, 418–419.
3 Q. Zhang, F. Wang, K. Jia and L. Kong, Natural Product Interventions for Chemotherapy and Radiotherapy-Induced Side Effects, *Front. Pharmacol.*, 2018, **9**, 1253.
4 S. Akbari-karadeh, S. Mahmoud, R. Aghamiri, P. Tajer-Mohammad-Ghazvini and S. Ghorbanzadeh-Mashkani, Radiolabeling of Biogenic Magnetic Nanoparticles with Rhenium-188 as a Novel Agent for Targeted Radiotherapy, *Appl. Biochem. Biotechnol.*, 2020, **190**, 540–550.
5 B. Bertrand, C. Botuha, J. Forté, H. Dossmann and M. Salmain, A Bis-Chelating/Ligand for the Synthesis of Heterobimetallic Platinum(II)/Rhenium(I) Complexes: Tools for the Optimization of a New Class of Platinum(II) Anticancer Agents, *Chem.–Eur. J.*, 2020, **26**, 12846–12861.
6 J. Liang, H. Zhong, G. Yang, K. Vellaisamy, D. Ma and C. Leung, Recent development of transition metal complexes with *in vivo* antitumor activity Pt, *J. Inorg. Biochem.*, 2017, **177**, 276–286.
7 P. Jia, R. Ouyang, P. Cao, X. Tong, X. Zhou and T. Lei, REVIEW: recent advances and future development of metal complexes as anticancer agents, *J. Coord. Chem.*, 2017, **70**, 2175–2201.
8 S. Dasari and P. Bernard, Cisplatin in cancer therapy: molecular mechanisms of action, *Eur. J. Pharmacol.*, 2014, **740**, 364–378.
9 S. Ghosh, Cisplatin: the first metal based anticancer drug, *Bioorg. Chem.*, 2019, **88**, 102925.
10 M. Masarik, M. Raudenska, J. Balvan, M. Fojtu and M. Masarik, Unexpected therapeutic effects of cisplatin, *Metallomics*, 2019, **11**, 1182–1199.
11 S. M. Cohen and S. J. Lippard, Cisplatin: From DNA Damage to Cancer Chemotherapy, *Prog. Nucleic Acid Res. Mol. Biol.*, 2001, **67**, 93–130.
12 A. Levina, D. C. Crans and P. A. Lay, Speciation of Metal Drugs, Supplements and Toxins in Media and Bodily Fluids Controls *In Vitro* Activities, *Coord. Chem. Rev.*, 2017, **352**, 473–498.
13 C. Santini, M. Pellei, V. Gandin, M. Porchia, F. Tisato, C. Marzano, T. Sez, U. Camerino, S. Agostino and U. Padova, Advances in Copper Complexes as Anticancer Agents, *Chem. Rev.*, 2014, **114**, 815–862.
14 D. Denoyer, S. Masaldan, L. Fontaine and M. A. Cater, Targeting Copper in Cancer Therapy: 'Copper That Cancer', *Metallomics*, 2015, **7**, 1459–1476.
15 A. Sharma, P. Sudhindra, N. Roy and P. Paira, Advances in novel iridium(III) based complexes for anticancer applications: A review, *Inorg. Chim. Acta*, 2020, **513**, 119925.
16 D. Ma, C. Wu, K. Wu and C. Leung, Iridium(III) Complexes Targeting Apoptotic Cell Death in Cancer Cells, *Molecules*, 2019, **24**, 2739.
17 A. Zamora, G. Vigueras, V. Rodríguez, M. D. Santana and J. Ruiz, Cyclometalated iridium(III) luminescent complexes in therapy and phototherapy, *Coord. Chem. Rev.*, 2018, **360**, 34–76.
18 A. T. Odularu, P. A. Ajibade and J. Z. Mbese, Impact of Molybdenum Compounds as Anticancer Agents, *Bioinorg. Chem. Appl.*, 2019, **2019**, 1–9.
19 P. Štarha and Z. Trávníc, Non-platinum complexes containing releasable biologically active ligands, *Coord. Chem. Rev.*, 2019, **395**, 130–145.
20 T. C. Johnstone, K. Suntharalingam and S. J. Lippard, The Next Generation of Platinum Drugs: Targeted Pt(II) Agents, Nanoparticle Delivery, and Pt(IV) Prodrugs, *Chem. Rev.*, 2016, **116**, 3436–3486.
21 N. Katsaros and A. Anagnostopoulou, Rhodium and its compounds as potential agents in cancer treatment, *Crit. Rev. Oncol. Hematol.*, 2002, **42**, 297–308.
22 P. Sudhindra, A. S. Sharma, N. Roy, P. Moharana and P. Paira, Recent advances in cytotoxicity, cellular uptake and mechanism of action of ruthenium metallodrugs: a review, *Polyhedron*, 2020, **192**, 114827.
23 S. Zhang, L. Gao, H. Zhao and K. Wang, Recent Progress in Polynuclear Ruthenium Complex-Based DNA Binders/ Structural Probes and Anticancer Agents, *Curr. Med. Chem.*, 2020, **27**, 3735–3752.
24 D. Gupta and M. Sathiyendiran, Rhenium-Carbonyl-Based Supramolecular Coordination Complexes: Synthesis, Structure and Properties, *ChemistrySelect*, 2018, **3**, 7439–7458.
25 C. C. Konkankit, S. C. Marker, K. M. Knopf and J. J. Wilson, Anticancer activity of complexes of the third row transition

metals, rhenium, osmium, and iridium, *Dalton Trans.*, 2018, **47**, 9934–9974.

26 K. M. Knopf, B. L. Murphy, S. N. Macmillan, J. M. Baskin, M. P. Barr, E. Boros and J. J. Wilson, *In Vitro* Anticancer Activity and *In Vivo* Biodistribution of Rhenium(I) Tricarbonyl Aqua Complexes, *J. Am. Chem. Soc.*, 2017, **139**, 14302–14314.

27 C. Tan, Y. M. Zhong, L. N. Ji and Z. W. Mao, Phosphorescent metal complexes as theranostic anticancer agents: combining imaging and therapy in a single molecule, *Chem. Sci.*, 2021, **12**, 2357–2367.

28 J. R. Shakirova, S. Nayeri, S. Jamali, V. Porsev, V. V Gurzhiy, O. V. Levin, O. Igor and S. P. Tunik, Targeted Synthesis of NIR Luminescent Rhenium Diimine cis,trans-[Re(N^N)(CO)2(L)2]n+ Complexes Containing N-Donor Axial Ligands: Photophysical, Electrochemical, and Theoretical Studies, *ChemPlusChem*, 2020, **85**, 2518–2527.

29 A. Leonidova and G. Gasser, Underestimated Potential of Organometallic Rhenium Complexes as Anticancer Agents, *Chem. Biol.*, 2014, **9**, 2180–2193.

30 P. Collery, A. Mohsen, A. Kermagoret, S. Corre, G. Bastian, A. Tomas, M. Wei, F. Santoni, N. Guerra, D. Desmaële and J. Angelo, Antitumor activity of a rhenium(I)-diselenoether complex in experimental models of human breast cancer, *Invest. New Drugs*, 2015, **33**, 848–860.

31 R. Ye, C. Tan, M. Chen, L. Hao, L. Ji and Z. Mao, Mono- and Dinuclear Phosphorescent Rhenium(I) Complexes: Impact of Subcellular Localization on Anticancer Mechanisms, *Chem.–Eur. J.*, 2016, **22**, 7800–7809.

32 M. Muñoz-Osses, F. Godoy, A. Fierro, A. Gómez and N. Metzler-Nolte, New organometallic imines of rhenium(I) as potential ligands of GSK-3β: synthesis, characterization and biological studies, *Dalton Trans.*, 2018, **47**, 1233–1242.

33 C. C. Konkankit, B. A. Vaughn, Z. Huang, E. Boros and J. J. Wilson, Systematically altering the lipophilicity of rhenium(I) tricarbonyl anticancer agents to tune the rate at which they induce cell death, *Dalton Trans.*, 2020, **49**, 16062–16066.

34 M. B. Ismail, I. N. Booysen and M. P. Akerman, DNA interaction studies of rhenium compounds with Schiff base chelates encompassing biologically relevant moieties, *Nucleosides, Nucleotides Nucleic Acids*, 2019, **38**, 950–971.

35 T. H. I. Ngoc, N. G. A. Tran, A. Mohsen and D. Desmaele, Dose Effect of Rhenium(I)-diselenoether as Anticancer Drug in Resistant Breast Tumor-bearing, *Anticancer Res.*, 2016, **36**, 6051–6058.

36 A. Subasinghe, I. C. Perera, S. Pakhomova and T. Perera, Synthesis, Characterization and Biological Studies of a Piperidinyl Appended Dipicolylamine Ligand and Its Rhenium Tricarbonyl Complex as Potential Therapeutic Agents for Human Breast Cancer, *Bioinorg. Chem. Appl.*, 2016, **2016**, 1–10.

37 P. Nunes, R. Morais, E. Palma, F. Silva, M. C. Oliveira, V. F. C. Ferreira, F. Mendes, L. Gano, H. V. Miranda, T. F. Outeiro and A. Paulo, Isostructural Re(I)/99mTc tricarbonyl complexes for cancer theranostics, *Org. Biomol. Chem.*, 2015, **13**, 5182–5194.

38 T. N. Aslan, E. Aşık and M. Volkan, Preparation and labeling of surface-modified magnetoferritin protein cages with a rhenium(I) carbonyl complex for magnetically targeted radiotherapy, *RSC Adv.*, 2016, **6**, 8860–8869.

39 D. Kaliba, M. Sticha and I. Jelinek, Synthesis and characterization of rhenium complexes of 1,2,3-trihydroxybenzene as potential antitumor agents, *Transition Met. Chem.*, 2017, **42**, 211–218.

40 B. Azadbakht, H. Afarideh, M. Ghannadi-Maragheh, A. Bahrami-Samani and M. Asgari, Preparation and evaluation of APTES-PEG coated iron oxide nanoparticles conjugated to rhenium-188 labeled rituximab, *Nucl. Med. Biol.*, 2017, **48**, 26–30.

41 K. Kowalski and U. Schatzschneider, Luminescent fac-[Re(CO)3(phen)] carboxylato complexes with non-steroidal anti-inflammatory drugs: synthesis and mechanistic insights into the *in vitro* anticancer activity of fac-[Re(CO)3(phen)(aspirin)], *New J. Chem.*, 2019, **43**, 573–583.

42 T. Tseng, S. Mendiratta, T. Luo and T. Chen, A new route to constructing rhenium(I)-based 8-hydroxyquinolate complexes: synthesis, structures and luminescent properties, *Inorg. Chim. Acta*, 2018, **477**, 312–317.

43 P. D. Asturias, Interligand C-C Coupling between α-Methyl N-Heterocycles and bipy or phen at Rhenium Tricarbonyl Complexes, *Inorg. Chem.*, 2017, **56**, 4249–4252.

44 J. J. Wilson, B. A. Vaughn and Z. Huang, rhenium(I) tricarbonyl anticancer agents to tune the rate at which they induce cell death, *Dalton Trans.*, 2020, **49**, 16062–16066.

45 A. K. Phosphorylation, I. Casari, S. Paternoster, W. Brian, M. Falasca and M. Massi, Defining the Anti-Cancer Activity of Tricarbonyl Rhenium complexes : Induction of G2/M cell cycle arrest and Blockade of Aurora-A Kinase, *Chem.–Eur. J.*, 2017, **23**, 6518–6521.

46 E. Dallerba, M. Massi and A. B. Lowe, Tetrazole functional copolymers: Facile access to well-defined Rhenium(I)-Polymeric luminescent materials, *Polymer*, 2020, **198**, 122522.

47 L. C. Lee, K. Leung, K. K. Lo and L. C. Lee, Recent development of luminescent rhenium(I) tricarbonyl polypyridine complexes as cellular imaging reagents, anticancer drugs and antibacterial agents, *Dalton Trans.*, 2017, **46**, 16357–16380.

48 M. S. Capper, H. Packman and M. Rehkämper, Rhenium-Based Complexes and *In Vivo* Testing: A Brief History, *ChemBioChem*, 2020, **21**, 2111–2115.

49 A. M. Yip and K. K. Lo, Luminescent rhenium(I), ruthenium(II) and iridium(III) polypyridine complexes containing a poly (ethylene glycol) pendant or bioorthogonal reaction group as biological probes and photocytotoxic agents, *Coord. Chem. Rev.*, 2018, **361**, 138–163.

50 A. Bjelosevic, B. J. Pages, L. K. Spare, K. M. Deo, D. L. Ang and J. R. Aldrich-wright, Exposing "Bright" Metals: Promising Advances in Photoactivated Anticancer Transition Metal Complexes, *Curr. Med. Chem.*, 2018, **25**, 478–492.

51 A. Shegani, C. Triantis, B. A. Nock, T. Maina, C. Kiritsis, V. Psycharis, C. Raptopoulou, I. Pirmettis, F. Tisato and

M. S. Papadopoulos, Rhenium(I) Tricarbonyl Complexes with (2- Hydroxyphenyl)diphenylphosphine as PO Bidentate Ligand, *Inorg. Chem.*, 2017, **56**, 8175–8186.

52 S. C. Marker, A. P. King, R. V. Swanda, B. Vaughn, E. Boros, S.-B. Qian and J. J. Wilson, Exploring ovarian cancer cell resistance to rhenium anticancer complexes, *Angew. Chem., Int. Ed.*, 2020, **59**, 13391–13400.

53 S. Imstepf, V. Pierroz, R. Rubbiani, M. Felber, T. Fox, G. Gasser and R. Alberto, Zuschriften Drug Targeting Organometallic Rhenium Complexes Divert Doxorubicin to the Mitochondria Zuschriften, *Angew. Chem., Int. Ed.*, 2016, **128**, 2842–2845.

54 C. Christina, P. Vasiliki, S. Xylouri, G. C. Kaiafas, M. Lazou and G. Bompola, Organometallic rhenium tricarbonyl–enrofloxacin and –levofloxacin complexes: synthesis, albumin-binding, DNA-interaction and cell viability studies, *JBIC, J. Biol. Inorg. Chem.*, 2019, **24**, 609–619.

55 L. He, Z.-Y. Pan, W.-W. Qin, Y. Li, C. Tan and Z. Mao, Impairment of the autophagy-related lysosomal degradation pathway by an anticancer rhenium(I) complex, *Dalton Trans.*, 2019, **48**, 4398–4404.

56 M. Muñoz-Osses, D. Siegmund, A. Gómez, F. Godoy, A. Fierro, L. Llanos, D. Aravena and N. Metzler-Nolte, Influence of the substituent on the phosphine ligand in novel rhenium(I) aldehydes. Synthesis, computational studies and first insights into the antiproliferative activity, *Dalton Trans.*, 2018, **47**, 13861–13869.

57 J. Yang, J. Zhao, Q. Cao, L. Hao, D. Zhou, Z. Gan, L. Ji and Z. Mao, Simultaneously Inducing and Tracking Cancer Cell Metabolism Repression by Mitochondria-Immobilized Rhenium(I) Complex, *ACS Appl. Mater. Interfaces*, 2017, **9**, 13900–13912.

58 E. E. Langdon-Jones, A. B. Jones, C. F. Williams, A. J. Hayes, D. Lloyd, H. J. Mottram and S. J. A. Pope, Anticancer, Azonafide-Inspired Fluorescent Ligands and Their Rhenium(I) Complexes for Cellular Imaging, *Eur. J. Inorg. Chem.*, 2017, **2017**, 759–766.

59 P. T. Wilder, D. J. Weber, A. Winstead, S. Parnell, T. V. Hinton, M. Stevenson, D. Giri, S. Azemati, P. Olczak, B. V. Powell, T. Odebode, S. Tadesse, Y. Zhang, S. K. Pramanik, J. M. Wachira, S. Ghimire, P. McCarthy, A. Barfield, H. N. Banerjee, C. Chen, J. A. Golen, A. L. Rheingold, J. A. Krause, D. M. Ho, P. Y. Zavalij, R. Shaw and S. K. Mandal, Unprecedented anticancer activities of organorhenium sulfonato and carboxylato complexes against hormone-dependent MCF-7 and hormone-independent triple-negative MDA-MB-231 breast cancer cells, *Mol. Cell. Biochem.*, 2018, **441**, 151–163.

60 J. Delasoie, A. Pavic, N. Voutier, S. Vojnovic, J. Nikodinovic-runic and F. Zobi, Identification of novel potent and non-toxic anticancer, anti-angiogenic and antimetastatic rhenium complexes against colorectal carcinoma, *Eur. J. Med. Chem.*, 2020, **204**, 112583.

61 G. Balakrishnan, T. Rajendran, K. S. Murugan, M. S. Kumar, V. K. Sivasubramanian, M. Ganesan, A. Mahesh, T. Thirunalasundari and S. Rajagopal, Thymus DNA: cytotoxic and cell imaging studies, *Inorg. Chim. Acta*, 2015, **434**, 51–59.

62 C. V. Garcia, L. Parrilha and L. Rodrigues, Tricarbonylrhenium(I) complexes with 2-acetylpyridine-derived hydrazones are cytotoxic to NCI-H460 human large cell lung cancer, *New J. Chem.*, 2016, **40**, 7379–7387.

63 C. C. Konkankit, B. A. Vaughn, S. N. Macmillan, E. Boros and J. J. Wilson, Combinatorial Synthesis to Identify a Potent, Necrosis-Inducing Rhenium Anticancer Agent, *Inorg. Chem.*, 2018, **58**, 3895–3909.

64 R. Ye, C. Tan, Y. Lin, L. Ji and Z. Mao, A phosphorescent rhenium(I) histone deacetylase inhibitor: mitochondrial targeting and paraptosis induction, *Chem. Commun.*, 2015, **51**, 8353–8356.

65 Z. -Y. Pan, C. -P. Tan, L. -S. Rao, H. Zhang, Y. Zheng, L. Hao, L. -N. Ji and Z. -W. Mao, Recoding the Cancer Epigenome by Intervening in Metabolism and Iron Homeostasis with Mitochondria-Targeted Rhenium(I) Complexes, *Angew. Chem., Int. Ed.*, 2020, **59**, 18755–18762.

66 Z. Pan, D. Cai and L. He, Dinuclear phosphoroscent rhenium(I) complexes as potential anticancer and photodynamic therapy, *Dalton Trans.*, 2020, **49**, 11583–11590.

67 K. M. Knopf, B. L. Murphy, S. N. Macmillan, J. M. Baskin, M. P. Barr, E. Boros and J. J. Wilson, *In Vitro* Anticancer Activity and *In Vivo* Biodistribution of Rhenium(I) Tricarbonyl Aqua Complexes, *J. Am. Chem. Soc.*, 2017, **139**, 14302–14314.

68 P. Collery, The rhenium(I) -diselenoether anticancer drug targets ROS, TGF- β1, VEGF-A and IGF-1 in an *in vitro* experimental model of triple-negative breast cancers, *Invest. New Drugs*, 2019, **37**, 973–983.

69 C. A. Kumar, R. Nagarajaprakash, W. Victoria, V. Veena, N. Sakthivel and B. Manimaran, Synthesis, characterisation and cytotoxicity studies of manganese(I) and rhenium(I) based metallacrown ethers, *Inorg. Chem. Commun.*, 2015, **64**, 39–44.

70 K. Ranasinghe, S. Handunnetti, I. C. Perera and T. Perera, Synthesis and characterization of novel rhenium(I) complexes towards potential biological imaging applications, *Chem. Cent. J.*, 2016, **10**, 71.

71 C. Concha, C. Quintana, A. H. Klahn, V. Artigas, M. Fuentealba, C. Biot, I. Halloum, L. Kremer, R. López, J. Romanos, Y. Huentupil and R. Arancibia, Organometallic tosyl hydrazones: synthesis, characterization, crystal structures and *in vitro* evaluation for anti-mycobacterium tuberculosis and antiproliferative activities, *Polyhedron*, 2017, **131**, 40–45.

72 L. D. Ramos, G. Cerchiaro and K. P. M. Frin, Rhenium(I) polypyridine complexes coordinated to an ethyl-isonicotinate ligand: luminescence and *in vitro* anti-cancer studies, *Inorg. Chim. Acta*, 2019, **501**, 119329.

73 S. C. Marker, S. N. Macmillan, W. R. Zipfel, Z. Li, P. C. Ford and J. J. Wilson, Photoactivated *In Vitro* Anticancer Activity of Rhenium(I) Tricarbonyl Complexes Bearing Water-Soluble Phosphines, *Inorg. Chem.*, 2018, **57**, 1311–1331.

74 S. C. Marker, A. P. King, S. Granja, B. Vaughn, J. J. Woods, E. Boros and J. J. Wilson, Exploring the *In Vivo* and *In Vitro* Anticancer Activity of Rhenium Isonitrile Complexes, *Inorg. Chem.*, 2020, **14**, 10285–10303.

75 A. P. King, S. C. Marker, R. V. Swanda, J. J. Woods, S. Qian and J. J. Wilson, A Rhenium Isonitrile Complex Induces Unfolded Protein Response-Mediated Apoptosis in Cancer Cells, *Chem.–Eur. J.*, 2019, **25**, 9206–9210.

76 G. Santoro, T. Zlateva, A. Ruggi and F. Zobi, Synthesis, characterization and cellular location of cytotoxic constitutional organometallic isomers of rhenium delivered on a cyanocobalmin scaffold, *Dalton Trans.*, 2015, **44**, 6999–7008.

77 I. Maisuls, E. Wolcan, O. E. Piro, E. E. Castellano, G. Petroselli, R. Erra-Balsells, F. M. Cabrerizo and G. T. Ruiz, Synthesis, Structural Characterization and Biological Evaluation of Rhenium(I) Tricarbonyl Complexes with β-Carboline Ligands, *ChemistrySelect*, 2017, **2**, 8666–8672.

78 B. S. Murray and P. J. Dyson, Recent progress in the development of organometallics for the treatment of cancer, *Curr. Opin. Chem. Biol.*, 2020, **56**, 28–34.

79 Z. Pan, D. Cai and L. He, Dinuclear phosphoroscent rhenium(I) complexes as potential anticancer and photodynamic therapy, *Dalton Trans.*, 2020, **49**, 11583–11590.

80 D. Giffard, E. Fischer-Fodor, C. Vlad, P. Achimas-Cadariu and G. S. Smith, Synthesis and antitumour evaluation of mono- and multinuclear [2+1] tricarbonylrhenium(I) complexes, *Eur. J. Med. Chem.*, 2018, **157**, 773–781.

81 R. Govindarajan, R. Nagarajaprakash, V. Veena, N. Sakthivel and B. Manimaran, One-pot reaction of amide functionalized Re(I) based dinuclear metallacycles: synthesis, characterization and evaluation for anticancer potential, *Polyhedron*, 2018, **139**, 229–236.

82 C. A. Kumar, D. Divya, R. Nagarajaprakasha, V. Veena, P. Vidhyapriya, N. Sakthivel and B. Manimarana, Self-assembly of manganese(I) and rhenium(I) based semi-rigid ester functionalized M_2L_2-type metallacyclophanes: synthesis, characterization and cytotoxicity evaluation, *J. Organomet. Chem.*, 2017, **846**, 152–160.

83 M. Redrado, I. Marzo and V. Ferna, Luminescent Re(I)/Au(I) Species As Selective Anticancer Agents for HeLa Cells, *Inorg. Chem.*, 2020, **59**, 8960–8970.

84 C. C. Konkankit, B. A. Vaughn, S. N. Macmillan, E. Boros and J. J. Wilson, Combinatorial Synthesis to Identify a Potent, Necrosis-Inducing Rhenium Anticancer Agent, *Inorg. Chem.*, 2019, **58**, 3895–3909.